A Search For Synthetic Lethality Between Polo-Like Kinase 3 and E-cadherin

JOEL GAASTRA

A thesis submitted in partial fulfillment of the requirements for the degree of

Bachelor in Biomedical Science with Honours
(Molecular Basis of Health and Disease)

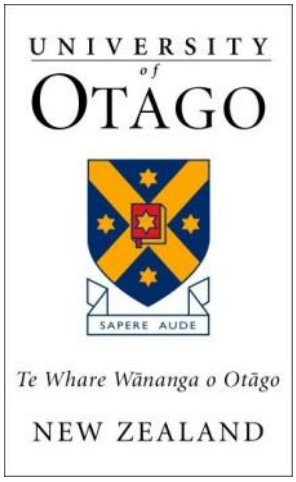

University of Otago
Dunedin, New Zealand

November 2015

ABSTRACT

Hereditary diffuse gastric cancer (HDGC) is an autosomal dominant condition caused by a mutation in the tumour suppressor gene E-cadherin, (*CDH1*). It predisposes to a 70% likelihood of developing highly penetrant diffuse gastric cancer[1]. Because HDGC is driven by the absence of a tumour suppressor, conventional therapeutic approaches targeting tumour-promoting oncogenes cannot be used. Synthetic lethality is an approach that circumvents this issue by targeting vulnerabilities in cells that lack the functional tumour suppressor. This project aimed to investigate a potential synthetic lethal relationship between *CDH1* and polo-like kinase 3 (*PLK3*), a cytoskeletal and cell cycle regulator.

Lentiviral delivery of two shRNA were successful in knocking down *PLK3* expression in isogenic MCF10A cell lines, with and without *CDH1* expression (MCF10A and $CDH1^{-/-}$) [2]. Viability was measured and confirmed as synthetic lethal (mutations in combination cause cells to be less viable) if the $CDH1^{-/-}$ cells were less viable with a ratio of ≤0.85. Results from one shRNA knockdown trended towards synthetic lethality ($p > 0.05$). Another shRNA resulted with a considerable reverse synthetic lethal effect, but was not statistically significant.

PLK antagonists poloxipan and wortmannin were used to inhibit PLK3 [3]. Poloxipan induced reverse synthetic lethality with reduced viability in MCF10A cells at low concentrations. High concentrations produced a

marginal synthetic lethal phenotype. Wortmannin's effect on MCF10A and *CDH1*$^{-/-}$ cells also varied from synthetic lethal and reverse synthetic lethal.

As the viability of *CDH1* deficient cells could not be significantly reduced via *PLK3* knockdown or inhibition, this candidate is no longer considered to be a potential therapeutic target for the treatment of HDGC.

ACKNOWLEDGEMENTS

This project has been a huge journey that has been contributed by a team of fantastic people who love their work.

First and foremost, the highest acknowledgements go to my eternal companion Mabel. She leads me by her example, having achieved so much. She sacrificed her highly demanded time to make sure I was undistracted and focused on this work. When things were failing, she talked me through it and has been the most consistent source of empathy and motivation.

Professor Parry Guilford is to thank for the tremendous opportunity this has been. No one has greater wisdom than this wizard of science. Thank you.

I am greatly indebted to my mentor, Bryony Telford. Countless hours, unorthodox late hour troubleshooting, training, direction, and proof reading is all thanks to you and I am earnestly grateful for all help and instruction you gave. Thank you for your patience!

Those in the Cancer Genetics Lab: Augustine, Henry, Andrew, Aziz, Liv, Kirsty, James, Tyler, Chris and Chris, Donghui, Kim, Grace, Anna, Jody, Adelaide, Tom, Sophie, Tanis, Anita, Rob, and Les, have given up much of their time, talents, and energies as service in contributing, guiding, counselling and supporting me or been part of the culture of excellence that this project was carried out in. You have my gratitude.

I also thank my parents; you set me on this path and have always been there for me. Thank you for your support.

To those who are burdened by cancer, my understanding does not know the weight of what you bear, but my heart goes out to you, and I dedicate this effort to you.

“Certanity of death, small chance of success…
What are we waiting for?” – Gimli, son of Glóin

TABLE OF CONTENTS

LIST OF FIGURES

LIST OF TABLES

ABBREVIATIONS

°C	Degrees Celcius
ATM	Ataxia Telangiectasia Mutated
bp	Base Pair
BRCA	Breast Cancer Susceptibility Gene
CDH1	Cadherin 1 (E-Cadherin) Gene
$CDH1^{-/-}$	MCF10A Cell Line With a *CDH1* Deletion
CO	Cell Only
Ct	Cycle Threshold
CTNNA1	Catenin (Cadherin-Associated Protein), Alpha 1
DAPI	Fluorescent Dye (4',6-Diamidino-2-Phenylindole)
DGC	Diffuse Gastric Cancer
DMEM	Dulbecco's Modified Eagle's Medium
DNA	Deoxyribonucleic Acid
dsRNA	Double-Stranded RNA
E-cadherin	Epithelial Cadherin
EGF	Epidermal Growth Factor

ER	Oestrogen Receptor
EtOH	Ethanol
F12	Ham's Nutrient Mixture F12
FBS	Foetal Bovine Serum
GFP	Green Fluorescent Protein
H&E	Hematoxylin And Eosin
HDGC	Hereditary Diffuse Gastric Cancer
HIF-1a	Hypoxia-Inducible Factor 1-Alpha
hrs	Hours
HS	Horse Serum
IDT	Integrated DNA Technologies
LB	Lysogeny Broth
LBC	Lobular Breast Cancer
MCF10A	Michigan Cancer Foundation-10 Attached Cell Line
MCF10F	Michigan Cancer Foundation-10 Floating Cell Line
MCF7	Michigan Cancer Foundation-7 Cell Line
min	Minutes
MOI	Multiplicity of Infection

MQ H_2O	Millipore Coporation Water
mRNA	Messenger RNA
NaOAc	Sodium Acetate
NE	No Enzyme
NI	No Insert shRNA
NS	Non-Silencing shRNA
NT	No Template
p53	Tumour Protein 53
PARP	Poly ADP Ribose Polymerase
PBS	Phosphate Buffer Saline
PES	Polyethersulfone
PI3K	Phosphoinositide 3-Kinase
PLK1	Polo-Like Kinase 1
PLK3	Polo-Like Kinase 3
psPAX2	Second Generation Packaging Vector
PTEN	Phosphatase And Tensin Homolog
RISC	RNA-Induced Silencing Complex
RNA	Ribonucleic Acid

Rnase	Ribonuclease
RT	Reverse Transcriptase
RT-qPCR	Real Time Quantitative Polymerase Chain Reaction
sec	Seconds
shRNA	Short Hairpin RNA
siRNA	Small Interfering RNA
TAE	Tris Base, Acetic Acid and EDTA Buffer Solution
TE	Tris and Ethylenediaminetetraacetic Acid
TU	Transducing Units
VSVG	Vesicular Stomatitis Virus Glycoprotein
WT	Wild Type

1 INTRODUCTION

1.1 HEREDITARY DIFFUSE GASTRIC CANCER

In this thesis a potential synthetic lethal partner of E-cadherin (*CDH1*) and cytoskeletal regulator, polo-like kinase 3 (*PLK3*) is targeted in *CDH1* deficient cells to aid in the investigation for a novel treatment for Hereditary diffuse gastric cancer (HDGC). HDGC was first coined after it was identified in three New Zealand Maori families with an autosomal dominant inheritance of diffuse gastric cancer [4]. HDGC is caused by a germ line genetic mutation in the E-cadherin gene (*CDH1*). Having a *CDH1* mutation leaves carriers with a 70% likelihood of developing diffuse gastric cancer and a 40% likelihood of developing lobular breast cancer [1,5].

Current clinical procedure for those who have a *CDH1* mutation is to conduct a total prophylactic gastrectomy. Removing their stomach has a highly adverse impact on the patient's quality of life and alternative treatments are needed[6]. *PLK3* has been identified as a therapeutic target in a high throughput small interfering RNA (siRNA) screen and needs to be investigated as to whether it can cause synthetic lethality in cases of HDGC.

1.1.1 IDENTIFICATION

HDGC was first identified in a New Zealand Maori family with heritable early onset gastric cancer. In 1964, a 21-year-old male came to hospital with inoperable carcinoma of the stomach. His cousin had died the year

before with the same condition. Tracing their family history back to the 1850s (**Figure 1**), cases of early onset gastric cancer were observed over three generations, with many dying at a young age [7].

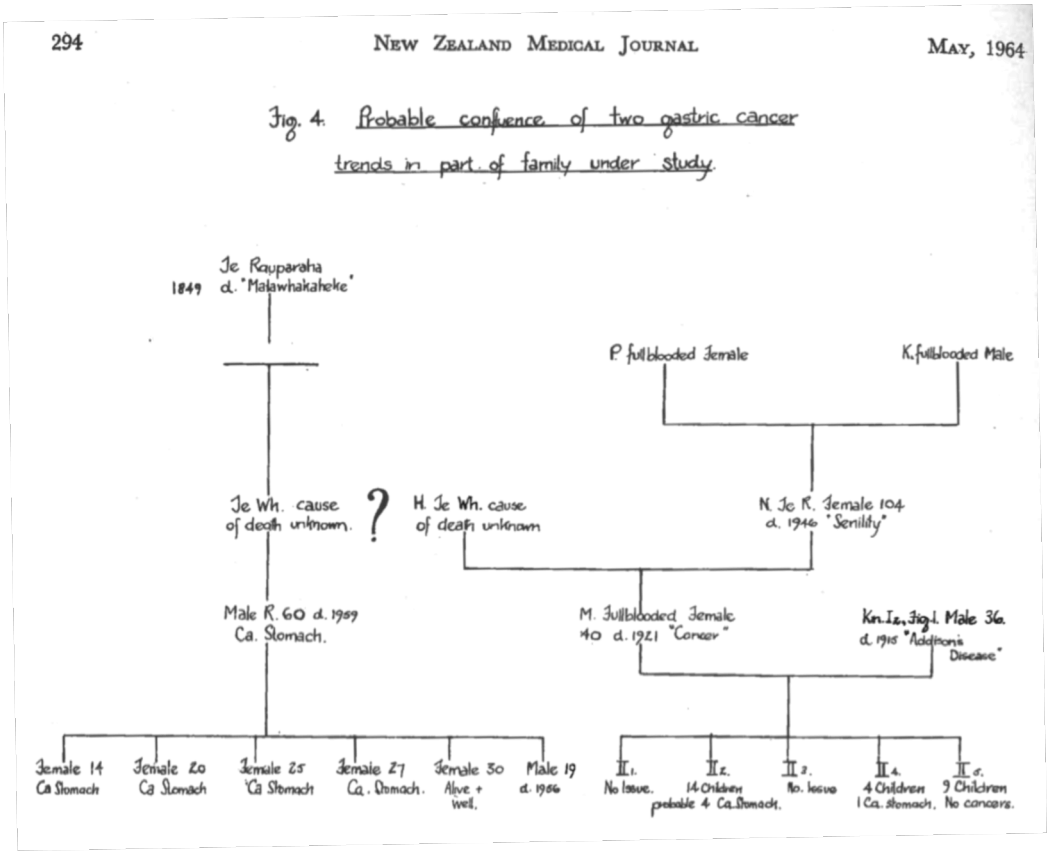

Figure 1 - Family pedigree showing HDGC. Cases of gastric cancer labelled Ca. stomach [7].

In 1998, a genetic linkage analysis was conducted on the same family. This allowed the tracking of their mutation to a genetic interval on chromosome 16q22.1 and the *CDH1* gene. Subsequent single stranded conformational polymorphism (SSCP) mutation analysis identified a band shift in exon 7 of the *CDH1* gene that was found in cases of diffuse gastric cancer from this family but was absent in 150 other unrelated chromosomes (1008G>T). This change affects one of the E-cadherin calcium binding pockets required

for the dimerization and the formation of rigid cell-to-cell adhesions and reduces splicing efficiency. This and other subsequently identified genetic alterations on *CDH1* render E-cadherin dysfunctional and prompted further research into HDGC and how it can be treated.

1.1.2 INCREASING AWARENESS OF HDGC

Gastric cancer is the third leading cause of cancer death worldwide with 70-85% of the 1 million individuals affected dying within 5 years of diagnosis. Lack of treatment options and late diagnosis contribute to this statistic, however further progress has been made in identifying HDGC cases because of increased genetic screening and identifying [8]. *CDH1* was identified as a cause of HDGC in 1998, resulting in additional families worldwide testing positive for *CDH1* mutations. There are now reports on over 104 unique *CDH1* mutations in cases of HDGC across many various ethnic origins (Table 1) [8].

Table 1 - Pathogenic germline defects in HDGC. Type, frequency and recurrence of *CDH1* and *CTNNA1* mutations [8]

Mutation Type	Frequency	Recurrence
CDH1		
Frameshift	39/104 (38%)	10/39 (26%)
Splice Site	24/104 (23%)	10/24 (42%)
Missense	18/104 (17%)	7/18 (39%)
Nonsense	18/104 (17%)	7/18 (39%)
Large Rearrangements	9/104 (9%)	4/9 (44%)
CTNNA1		
Frameshift	1/1	NA

Identification of *CDH1* mutations in multiple families aided with understanding of HDGC and tumour development. Onset of HDGC begins

after a second hit on the *CDH1* gene abrogates all E-cadherin expression [9,10]. In accordance with the Knudson hypothesis, the first hit is the inheritance of a mutated *CDH1* allele, whilst still having a functional copy of *CDH1* in the other allele [11]. Hyper-methylation of the *CDH1* promoter region silences the second *CDH1* allele in over 50% of cases of HDGC. This silencing is the second hit, leaving the carrier with a total loss of E-cadherin. Some report as high as 83% of diffuse gastric cancer cases have hyper-methylation of the *CDH1* promoter and can occur regardless of whether *CDH1* itself is mutated or not [10,12,13].

As shown by the failure to identify *CDH1* mutations in some HDGC families, not all familial gastric cancer cases are explained by *CDH1* mutations and *CDH1* methylated silencing [5,14-17]. The *CTNNA1* gene that codes for α-catenin was identified in 2013 in one HDGC family (Table 1) [18]. α-Catenin is part of the cytoskeleton structure that binds to E-cadherin forming stable adherens junctions. This identification is further evidence of the important association between the cytoskeletal structures and the adherens junction. Having a biologically plausible target that is vulnerability for the development of novel synthetic lethal therapeutic treatments such as targeting *PLK3* [15].

1.1.3 MANAGEMENT OF HDGC

After identifying *CDH1* mutations in HDGC, a protocol was created by the International Gastric Cancer Linkage Consortium for the guidance of medical professionals working with HDGC [19,20]. A clinical and psychosocial benefit results from family members knowing if they have inherited the defective *CDH1* gene because carriers have a 70% likelihood of developing an aggressive diffuse gastric cancer [1,19]. Biopsies are the current gold standard of pathological diagnosis. The major distinguishing pathological features of diffuse gastric cancer are the signet-ring cell carcinomas, evident in H&E staining as cells with a large vacuole that contains the glycosylated mucin proteins (**Figure 2**) [21]. Signet-ring cell carcinomas in the biopsy are a key indicator that strongly indicates gastrectomy as treatment [22].

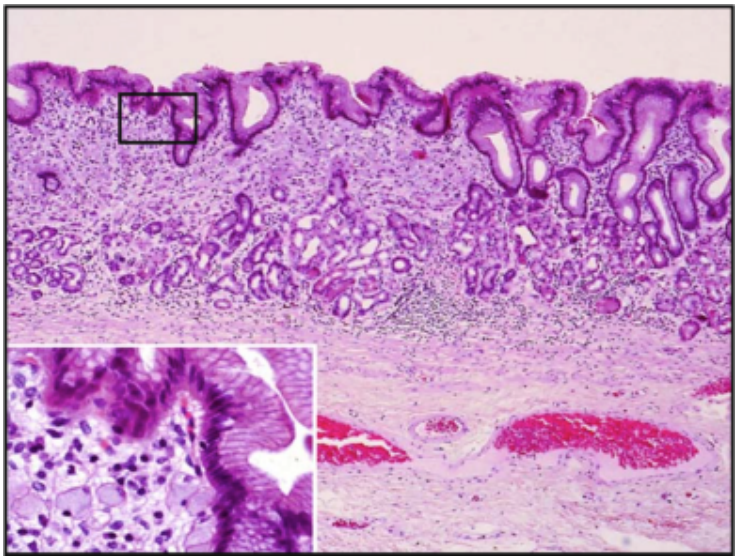

Figure 2 - Stage T1a signet ring cell carcinoma from a CDH1 germline mutation carrier. The 9-mm focus (occupying the left two-thirds of the frame) occupies the full thickness of the mucosa under an intact epithelium (H&E, ×40). The inset frame shows signet ring cells in the lamina propria at ×400 [22].

When a patient has tested positive for a germline *CDH1* mutation, carriers are then presented with the only guaranteed preventative of diffuse gastric cancer, a total prophylactic gastrectomy. The alternative is to continue to be monitored by biopsies. [13,19,20,23]. The carrier then holds in consideration the prevalence of developing diffuse gastric cancer with a likelihood of 70% or a new life without a stomach. The operation itself has a mortality rate of 1-2%, leads to morbidity, dramatic weight loss, and restrictive diets that impact their quality of life. Patients also infrequently suffer from oesophagitis and women with the mutation will still have the increased risk of developing lobular breast cancer [6,24]. Prophylactic gastrectomy prevents diffuse gastric cancer but the high cost of this procedure makes investigation into alternative measures essential.

1.2 E-CADHERIN AND POLO-LIKE KINASE 3

E-cadherin (*CDH1*) is a calcium-dependent cell-cell adhesion protein of the adherens junction. E-cadherin maintains cell polarity, connects to the cytoskeleton and is a regulator of cell signalling. E-cadherin was the first of the cadherin family to be discovered so that there is a comprehensive but incomplete understanding of its role in the cell [25]. Further research will be beneficial to understanding E-cadherin's role as a tumour suppressor and driver of diffuse gastric cancer and lobular breast cancer [26].

In a siRNA screen, conducted by our laboratory polo-like kinase 3 (*PLK3*) was found to be in a synthetic lethal relationship with *CDH1* (Table 2, **Figure 3**) [27]. The synthetic lethal treatment concept is applicable in

tumour suppressor cases such as HDGC. A synthetic lethal partner of *CDH1* such as *PLK3* can then be targeted to cause cell death only in *CDH1* mutant tumour cells. If the two genes are in a synthetic lethal partnership, the mutated *CDH1* cancer cells will die, while the non-mutated *CDH1* cells remain viable.

Table 2 - Viability of MCF10A and CDH1-/- cells from the siRNA screen. Measured 24 hours (hrs) after treatment for luminescence value to reflect the amount of viable cells. The treatments were normalised to a mock siRNA and compared for a viability ratio. The threshold to be considered a synthetic lethal relationship was a viability ratio of ≥0.85 and was seen in the original pool of siRNA, siRNA2 and siRNA4.

Viabilty from siRNA Screen			
	MCF10A	*CDH1*$^{-/-}$	Viability Ratio
siRNA1	0.92	0.82	0.89
siRNA2	0.68	0.52	0.76
siRNA3	0.62	0.68	1.10
siRNA4	0.66	0.52	0.79
Pool of siRNA	0.90	0.76	0.84

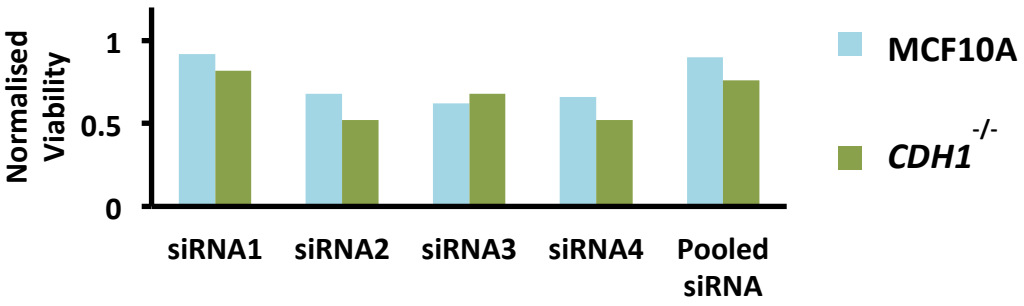

Figure 3 - Viability of the MCF10A and *CDH1*$^{-/-}$ cells from the high throughput screen of siRNA Cells were treated with four individual siRNA sequences that targeted the knockdown *PLK3* mRNA. After 24 hrs the luminescence determined the amount of cells and the siRNA value was normalised to the average of the siRNA mock control. The threshold to be considered a synthetic lethal relationship was a viability ratio of ≥0.85 and was seen in the original pool of siRNA, siRNA2 and siRNA4.

PLK3 is a serine/threonine-protein kinase that serves as a cyto-skeletal regulator and cell cycle regulator. Specifically, PLK3 interacts with the spindle poles during mitosis. It also functions as a tumour suppressor causing cell cycle arrest in response to a variety of stress conditions such as genetic damage or hypoxia [28]. It is of great interest to validate whether a *CDH1* mutation and the knock down of *PLK3* will induce the synthetic lethal effect, because of the tumour suppressor properties of *PLK3*.

1.2.1 DISCOVERY AND ROLE OF E-CADHERIN

The first report of E-cadherin came after discovery that $Ca2^{+}$ in the presence of a 150kDa sized surface protein was able to protect cells from trypsinization by maintaining increased adhesion [29]. E-cadherin was first named uvomorulin after anti-uvomorulin antibodies impaired a mouse morula, rendering the structure to resemble uva (Latin for grapes) [30].

Eventually a discrepancy was identified in the effects of antibodies that inhibited adhesion on a 68kDa protein in liver cells, but were not able to cause similar inhibition of adhesion in retinal cells. Another antibody that inhibited epithelial cell adhesion was ineffective against adhesion of fibroblastic cells. New antibodies were developed that were able to specifically inhibit the cell-cell adhesion in the fibroblasts and for other tissues and these proteins became known as “cadherins” after their tissue type (E for epithelial cadherin) [31,32].

E-cadherin, as a member of the cadherin superfamily, is a calcium dependent cell-cell adhesion glycoprotein coded for at position q22.1 on

chromosome 16 of homo sapiens [25]. It has a cytoplasmic domain, a transmembrane domain, and an external E-cadherin domain. The external E-cadherin domain consists of five repeat domains, the fifth domain being distinguishable by four cysteines. This fifth domain is reduced to form strong disulphide bridges with a neighbouring cell's fifth extracellular domain, forming cell-cell adhesion. The cytoplasmic domain has become a great point of interest in research recently because of its involvement in many other pathways, such as involving the WNT pathway, Rho GTPase , multiple catenins, myosins, F-actin and various other cell skeleton constituents (**Figure 4**) [33-35]. Contributing to these pathways E-cadherin loss/mutation has the potential to affect a range of processes ultimately leading to HDGC.

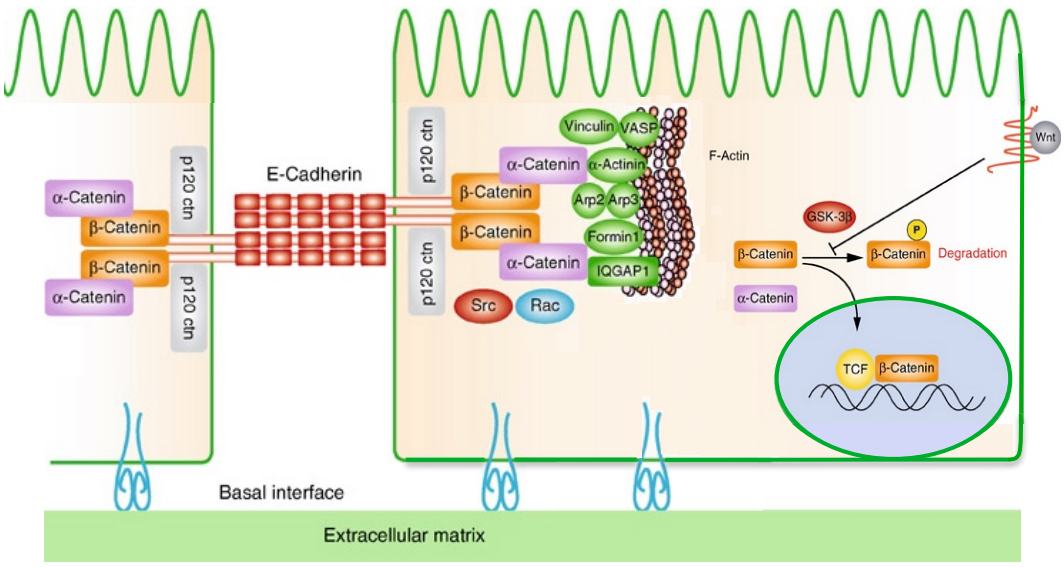

Figure 4 – E-cadherin function. The junction between two neighbouring epithelial cells and the various integrations of cytoskeletal structures and regulatory proteins [36].

1.2.2 TREATING E-CADHERIN DEFICIENT CELLS

E-cadherin is a tumour suppressor lost in the early stages of gastric and breast cancer and an invasion suppressor lost in the late stages of various other cancer types. Cancer inducing somatic *CDH1* mutations were identified in diffuse gastric cancer before the discovery of germline *CDH1* mutations [37]. These sporadic cases had a truncated E-cadherin due to somatic mutations causing exon skipping. Additionally, other tissue types may down-regulate or have mutant *CDH1* allowing for late invasive abilities in bladder, colon, lung, oesophagus, ovary and thyroid carcinomas but germline mutations of *CDH1* in these cancers are very rare [25,38]. E-cadherin loss initiates gastric and breast cancer formation by loss of the cell's polarity and adhesion (**Figure 2**). It is important to target the vulnerabilities this loss provides before the diffuse gastric cancer tumour advances.

When a tumour suppressor such as *CDH1* becomes mutated and does not function normally, it leads to the formation of a tumour. Directly targeting the mutated tumour suppressor is not possible, because unlike a cancer causing oncogenic protein, it is the absence of the tumour suppressor gene that causes cancer in this case. An example of targeting an oncogene is the overactive oestrogen receptor in breast cancer. This oncogene promotes the cancer growth and is targetable with a treatment of and inhibitor, anti-oestrogen drug tamoxifen [39]. For cases with *CDH1* tumour suppressor loss, it is not possible to target the cause, as the protein is already lost.

Therefore another treatment target other than the causal mutation (*CDH1*) is needed.

One such treatment strategy is termed synthetic lethality; a proven concept where a second allelic trait is considered a synthetic lethal partner of the first trait (*CDH1*). The two traits are compatible with life separately, but a combination of loss of both traits is lethal (**Figure 5**). The synthetic lethal technique is used in cancer treatments when tumour targets are absent (such as *CDH1*) due to the mutation inactivating a tumour suppressor gene. This loss becomes the first trait that will make it vulnerable to the targeting of its synthetic lethal partner [40].

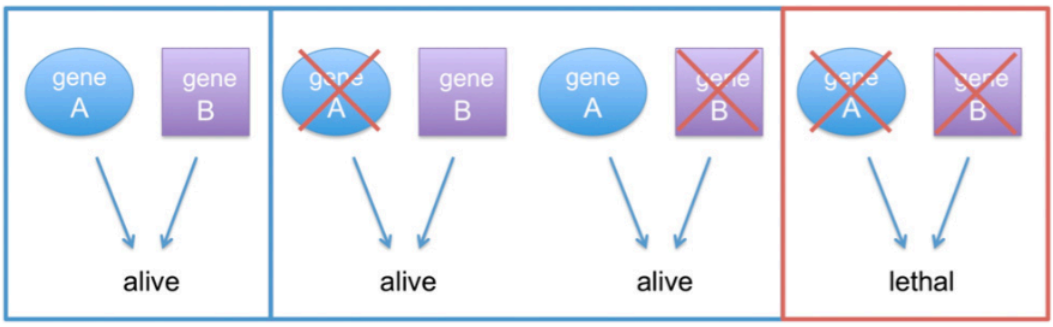

Figure 5 - Synthetic lethality. Two genes are synthetic lethal only when their simultaneous inactivation results in cellular or organismal death. In this example, deletion of either gene A or gene B does not affect viability whereas inactivation of both at the same time is lethal [40].

A great example of where this technique is currently in clinical use is with *BRCA* mutations and poly ADP-ribose polymerase (PARP) inhibitors. PARP inhibitors provide a synthetic lethal hit to *BRCA* mutated cells [41]. Tumour suppressors BRCA1 and BRCA2 are DNA repair proteins. DNA damage would accumulate without functioning BRCA proteins, and cells with this mutation are prone to further oncogenic mutations allowing for tumour

growth [42]. PARPs are also involved in repair of DNA, repairing single-stranded breaks. It was found that PARP inhibition has a lethal effect in cells with *BRCA* mutations but does not cause any significant loss in WT cells that have functioning BRCA [43]. Synthetic lethality caused by PARP inhibitors continues to be a successful treatment strategy, inspiring multiple other efforts to find targeted synthetic lethal combinations for other tumour suppressor mutations such as with *CDH1*.

A high throughput screen conduced in our laboratory using a siRNA library on a MCF10A breast cancer cell line and its isogenic partner (MCF10A with a *CDH1*$^{-/-}$ deletion referred to hereafter as *CDH1*$^{-/-}$) identified various synthetically lethal candidates [2,27]. Each pool of four siRNAs would specifically targeted the knockdown of one out of 18,120 genes in MCF10A and *CDH1*$^{-/-}$ cells. A gene was considered to be a synthetically lethal partner of *CDH1* if the ratio of *CDH1*$^{-/-}$ cell viability over MCF10A viability was ≤0.85. *PLK3* was one of the candidates making these thresholds. The viability of the MCF10A cells was 0.90 after the *PLK3* knockdown and the viability of the *CDH1*$^{-/-}$ cells was 0.76. This provided a viability ratio of 0.84. In the secondary screen, *PLK3* was amongst 500 gene candidates that had the shRNA pool de-convoluted to test the four-pooled siRNAs individually. Of the four siRNAs targeting *PLK3*, 2 out of 4 were above the standards to be considered synthetically lethal. Another factor that promotes *PLK3* as a synthetic lethal partner of *CDH1* is PLK3's biological relevance as a tumour suppressor and its interactions with E-cadherin.

1.2.3 POLO-LIKE KINASE 3

Polo-like kinases are a family of kinases that regulate the cell cycle. They all have an amino-terminal serine/threonine kinase catalytic domain and distinguishing polo box domains [44]. Polo-like kinase 1 (*PLK1*) is a research validated therapeutic cancer target that induces cell death. *PLK3* however is not as well understood [45,46]. The similarity of all the PLKs allows them to be targeted by similar inhibitors with varying and currently undetermined quantification. This casts a shadow on this therapeutic research, as PLK1 inhibitors are not specific to PLK1 and some of the anti-cancer therapeutic effects could be attributed to the inhibition of other PLKs [47]. PLK inhibitors are currently undergoing clinical trials, despite their off target inhibition not yet being well characterised. This is not unusual for drug therapies.

The subtle difference in each PLK gives these kinases a unique functional role. Upon DNA damage, ataxia telangiectasia mutated (ATM) indirectly causes phosphorylation of PLK3. This relationship is not a directly phosphorylation but PLK3 is dependent on ATM's presence [48]. PLK3 will however directly phosphorylate p53, allowing for activation of cell cycle arrest and apoptosis if the signal is sustained in situations of excessive DNA damage. PLK3 activates cell cycle arrest via activation of CHK2 that will then acts at the G2/M transition, and inhibits CDC25, an activator of cell cycle progression (**Figure 6**) [48-51]. Despite the lack of a complete association at every step, the evidence that implicates *PLK3* as a tumour

suppressor is strong. The gaps in our knowledge regarding the associations of *PLK3* make it difficult to predict the effects of targeting this kinase.

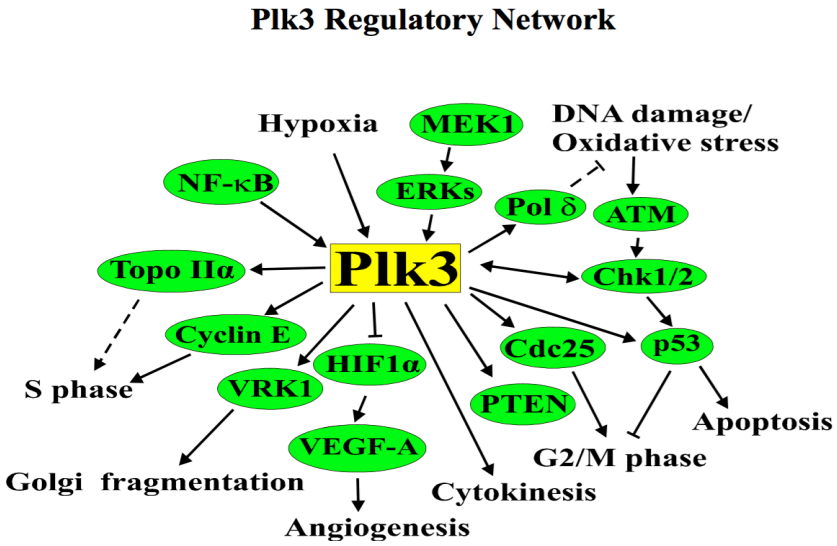

Figure 6 - Known tumour suppressor functions of PLK3. *PLK3* regulates a number of cellular activities by modulating a wide array of cellular components. Arrows indicate activation and T-bars indicate inhibition.

PLK3 shows other tumour suppressor qualities such as activating DNA repair and inhibiting angiogenesis (**Figure 6**). It is proven to associate with and cause phosphorylation of DNA repair polymerase δ, in combination with previously mentioned cell cycle arrest. This allows DNA repair to occur, resulting in fewer mutations accumulating with each cell division [49]. Expression of hypoxia-inducible factor 1-alpha (*HIF-1α*) is often increased in tumours as the growth of a tumour renders a state of hypoxia due to the lack of blood supply. HIF-1α initiates angiogenesis so that oxygenated blood can be delivered to the oxygen deprived tumour cells, allowing for further tumour growth. PLK3 acts as a tumour suppressor by directly phosphorylating HIF-1α, causing it to be destabilized and

repressed [52]. PLK3 also phosphorylates and stabilises PTEN, which then inhibits HIF-1α [28,52,53].

However, these tumour suppressor characteristics are not associated with E-cadherin. PLK3 is relevant to E-cadherin in that it is a regulator of the cell cytoskeletal network. Inactivation of PLK3 causes disruption of the cytoskeletal structures and can lead to apoptosis. PLK3 has been identified accumulating around centrioles and the cells spindle poles during metaphase by immunofluorescence imaging of cells during mitosis. During telophase, PLK3 accumulates by the mid-body where cytokinesis is occurring [54]. PLK3 over-expression causes a shrunken conformation of cells with a more rounded morphology.

Knockdown of *PLK3* by RNA inhibition with short hairpin RNA (shRNA) and a non-functional *PLK3* mutant causes microtubule structures to be elongated and protrude through cell walls with an increase of apoptosis [54-56]. Other findings confirm this pattern, with activated PLK3 forming complexes with un-polymerized tubulin, promoting its formation. *PLK3* inhibition causes incomplete cytokinesis, multinucleated division, Golgi fragmentation causing "mitotic catastrophe" and apoptosis (**Figure 7**) [47,48,51,55,57]. It is expected that the increased lethality observed in *CDH1*$^{-/-}$ cells is due to an increased vulnerability to cytoskeletal structures penetrating the cell membrane and causing mitotic catastrophe.

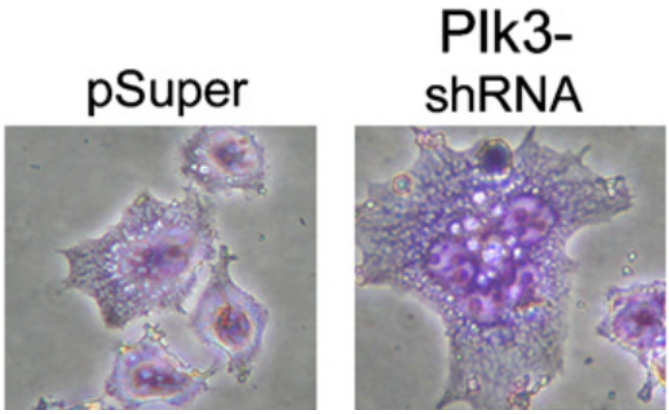

Figure 7 - T47D cells with *PLK3* knockdown by shRNA. Knockdown causes apoptosis and multinucleated cells compared to the plasmid vector [57].

Yet to be identified is any direct interaction between *PLK3* and E-cadherin that gives biological plausibility to the hypothesis that *CDH1*$^{-/-}$ cells will be synthetically lethal with *PLK3* knockdown or inhibition.

1.3 EXPERIMENTAL AIM

The aim of this project is to validate any synthetic lethality when *PLK3* is targeted in MCF10A cells. *PLK3* expression will be knocked down using shRNA (an alternative to the siRNA used in the high throughput screen). PLK3 will also be inhibited using current non-specific PLK inhibitors poloxipan and wortmannin targeting PLK proteins in MCF10A and *CDH1*$^{-/-}$ cells. The outcomes of this study will impact further research efforts in finding a treatment to prevent HDGC and provide further insights on the effects of PLK inhibition.

1.4 EXPERIMENTAL BACKGROUND

1.4.1 LENTIVIRAL SHRNA

The original high throughput screen was conducted using siRNAs as a means of inhibiting protein expression and this needs to be validated using alternatives such as short hairpin RNAs (shRNAs) [27]. Small interfering RNAs (siRNAs) are chemically synthesized and double stranded whereas shRNAs are continually expressed from the cell after a vector is inserted into the cell DNA [58]. In order to be incorporated into the cell, an envelope protein and a packaging vector create the virus and are assembled to contain the shRNA plasmid vector by being assembled during transfection in 293FT cells. The envelope protein of the virus we use is vesicular stomatitis viral glycoprotein (VSVG) and the packaging vector is psPAX2. psPAX2 contains RNA polymerase III, reverse transcriptase (RT), integrase and protease which help the shRNA incorporate to the DNA of the host and facilitate expression. The shRNA is part of a GIPZ transfer plasmid that also contains green fluorescent protein (GFP) and antibiotic resistance proteins.

After an shRNA vector is incorporated into a cell, shRNA is synthesized in the nucleus, and then modified by Drosha and Dicer protein complexes. This prepares the pre-shRNA for the RNA-induced silencing complex (RISC) which has an Argonaute endonuclease subunit that primes the shRNA to target the shRNA's complementary mRNA and cleave it (**Figure 8**) [59,60]. In this manner, mRNA is cleaved and degraded, which prevents the target gene from being translated into protein.

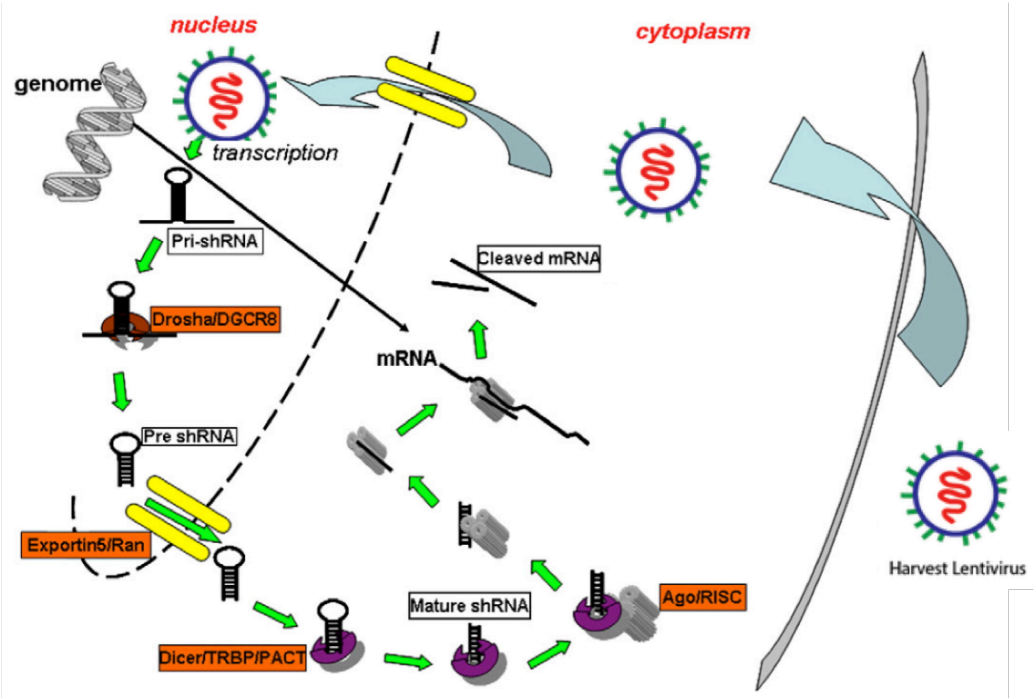

Figure 8 - The course of shRNA into the nucleus and subsequent processing to cleave the mRNA. Drosha, Exportin5, Dicer and RISC protein complexes contribute to produce functional shRNA with the ability to cleave the target mRNA [61].

The loading of siRNA to RISC is reported as 10x less effective than that of shRNA. 48 hrs post transduction; siRNA is reported to degrade so that less than 1% of the introduced double stranded duplex remains. shRNA however is continuously expressed by the host cell making the shRNA knockdown more durable [61]. These weaknesses in siRNA promote shRNA as a more reliable mechanism to carry out RNA interference.

The high transfection efficiency and integration of exogenous DNA of the lentiviral vector delivery system promotes shRNA as the preferable method of RNA interference. shRNA is introduced via lentiviral vector transduction, along with lipofectamine, psPAX2 as a packaging vector, and the G glycol-protein of the rhabdovirus vesicular stomatitis virus (VSVG) as an envelope

protein that aids in transfection efficiency by forming fusogenic liposomes [62-64]. This particular method has been considered dangerous to laboratory personnel in the past. Further reviews promote their use as safe in a secure lab environment, but should never have a clinical use [61,65]. They do however provide a great tool that can identify therapeutic targets that can aid cancer research.

1.4.2 MCF10A CELLS WITH AND WITHOUT *CDH1* EXPRESSION

The MCF10A cell line was named after the Michigan Cancer Foundation, the institute that isolated it. The spontaneously immortalised MCF10A (A for attached) cell line is from a 36-year-old woman who had no family history of breast cancer. MCF10A cells are non-tumorigenic, do not require a pro-carcinogen, have no SV40 genetic material, and the karyotype is near-diploid with minimal rearrangement [66]. MCF10As are limited as a model of mammary epithelial cells as they need to be organised into a three-dimensional basement membrane to be a true replicate of pathogenesis, but they are sufficient models for providing proof of principle of a synthetic lethal effect [67].

An isogenic MCF10A *CDH1*$^{-/-}$ cell line was created via zinc finger nuclease (Sigma-Aldrich). The knockout of *CDH1* was caused by a 4 bp homozygous deletion in exon 11 resulting in a frameshift, a premature stop codon, and a truncated E-cadherin protein that was confirmed by immuno-fluorescence.

The *CDH1*$^{-/-}$ cells have the following characteristics: a rounder morphology, less dense microtubule network and slower migration time [2]. One

confounding factor in all future comparisons between these two cell lines is that the *CDH1*$^{-/-}$ cells have a significant change in gene expression. This includes an expected compensating upregulation of desmosomes, tight junctions and gap junction genes because of the deficiency of E-cadherin in forming adherens junctions [2]. Further research on other models will be needed to validate any synthetically lethal combinations that occur on the MCF10A cells with and without *CDH1* expression, especially considering that HDGC occurs in gastric as well as breast cells.

1.4.3 POLOXIPAN

Polo-like kinases interact with the cyclin-dependent kinases and Aurora kinases in regulation of the cell cycle and as such, small molecule inhibits for PLK1 were identified. PLK1 binds directly with p53, causing the tumour suppressor to degrade. PLK1 also reduced the activity of other pro-apoptotic proteins: p21, p73 and BAX [47]. PLK1 inhibitors are therefore a plausible and valid solution to several cancers. There are current PLK1 inhibitors in clinical development, which is controversial due to research that shows they also inhibit PLK2 and PLK3 at similar concentrations.

As research continues to indicate that PLK3 is a tumour suppressor, it is concerning that PLK1 inhibitors are be limiting PLK3s tumour suppressor role. Poloxipan is a pan-specific PLK inhibitor that is not in any current clinical trials. Poloxipan's IC_{50} for PLK1 is 3.2μM, and for PLK3 it is 3.0μM [3]. Out of the many PLK inhibitors, this one was the only one to show more inhibition for PLK3 than for PLK1 as most research is aimed at avoiding

inhibition of PLK3. Poloxipan is currently the most suitable PLK3 protein inhibitor to investigate if PLK3 is in a synthetic lethal relationship with E-cadherin.

1.4.4 WORTMANNIN

Wortmannin is a well-characterised Phosphoinositide 3-kinase (PI3K) inhibitor that is used as an in vivo anti-tumour therapy studies [68]. Although wortmannin is a potent PI3K inhibitor it is shown to inhibit a broad range of substrates including PLK1 and PLK3 at the concentrations that it would be used to inhibit PI3K. The IC50 values for PI3K are reported to be at 3nM and for PLK3 were 48nM [69].

1.5 HYPOTHESIS

We hypothesize that *PLK3* is a synthetic lethal partner of *CDH1*. Targeting *PLK3* is predicted to reduce the viability of *CDH1*$^{-/-}$ cells while MCF10A cells will remain viable.

1.6 EXPERIMENTAL OVERVIEW

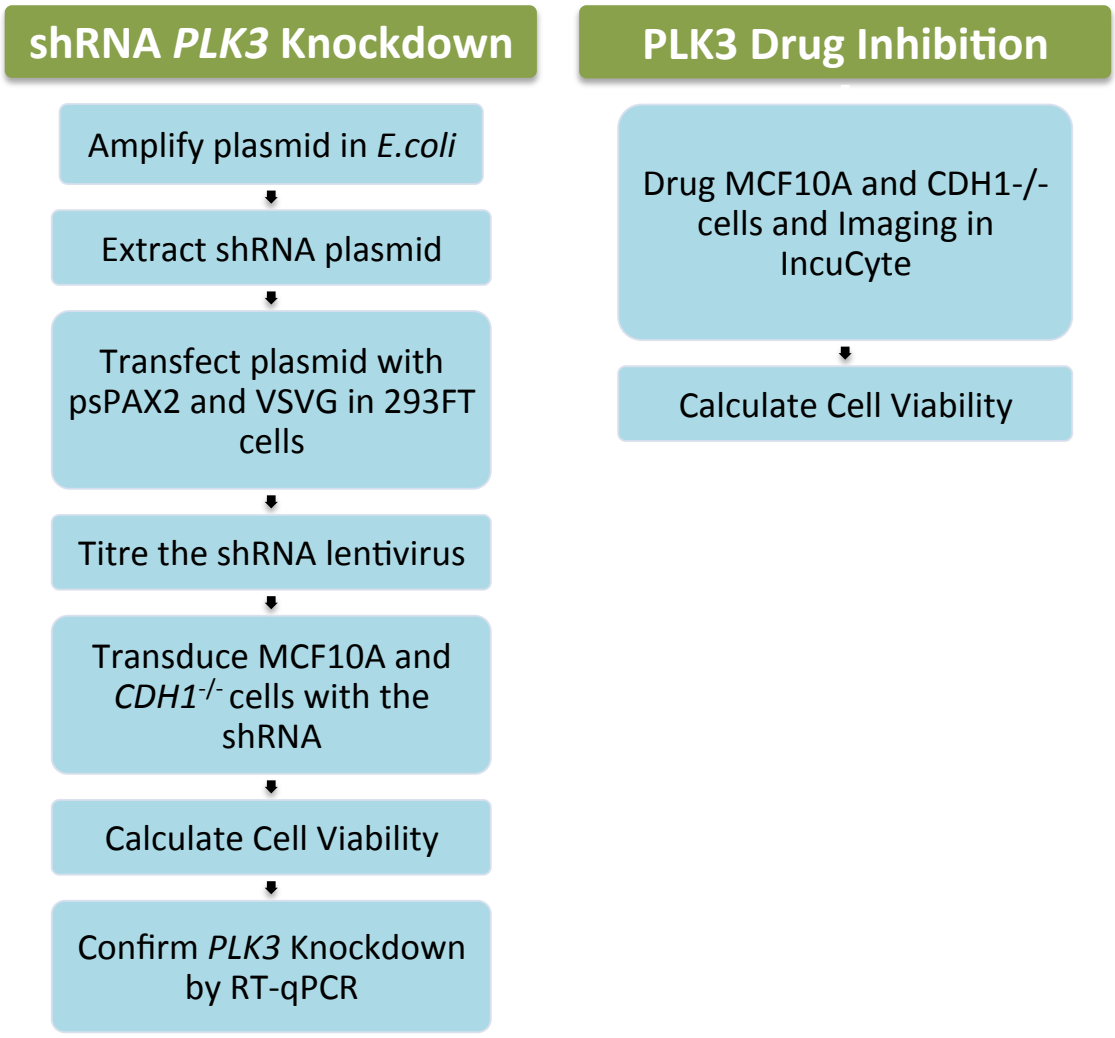

2 METHODS

"Just keep trying" – Jeffrey R Holland

2.1 MATERIALS

2.1.1 REAGENTS

The water used in all experiments was ultrapure water of "Type 1" quality (resistivity 18.2MΩ·cm at 25°C) prepared using a Millipore Corporation water filtration station.

0.05% Trypsin Solution

293FT Cell Line – Donated Dr S. Hughes, NZ

Agar (A0949) – AppliChem, USA

Ampicillin – Sigma-Aldrich, USA

CDH1$^{-/-}$ Cell Line – Sigma-Aldrich, USA

Cholera Toxin – Sigma-Aldrich, USA

Dimethyl Sulfoxide (DMSO) – Sigma-Aldrich, USA

Dulbecco's Modified Eagle's Medium (DMEM) – Invitrogen, USA

Dulbecco's Modified Eagle's Medium and F12 Medium (DMEM-F12) – Invitrogen, USA

Ethanol (EtOH) – Lab Supplies, NZ

Foetal Bovine Serum (FBS) – Invitrogen, USA

Glycerol – Scharlau, Australia

Hoechst 33342 Dye – Sigma-Aldrich, USA

Horse Serum – Invitrogen, USA

Human Epidermal Growth Factor (EGF) – PeproTech, USA

Hydrocortisone – Sigma- Aldrich, USA

Insulin (Actrapid® Penfill® 100iu/mL) – Novo Nordisk®, Denmark

KAPA SYPR FAST RT-qPCR Kit – Kapa Biosystems, South Africa

Kapa Universal DNA Ladder - Kapa Biosystems, South Africa, USA

L-Glutamine – Invitrogen, USA

Lipofectamine® 2000 Transfection Reagent – Life Technologies, USA

Lysogeny Broth (LB) – Prepared In Lab (Appendix 5.3.2)

MCF10A Cell Line – Sigma-Aldrich, USA

Non-Essential Amino Acids – Invitrogen, USA

Opti-MEM – Life Technologies, USA

Paraformaldehyde – VWR Chemicals, NZ

pGIPZ shRNA PLK3, Non-Silencing And No Insert Constructs – Dharmacon, USA

Phosphate Buffered Saline (Dulbecco A) Tablets – Oxoid Limited, UK

Poloxipan – Vitas-M Laboratory, Hong Kong

PrimeScript RT Reagent Kit (Perfect Real Time) – TAKARA BIO INC., Japan.

Propidium Iodide – Thermo Fisher Scientific, USA

psPAX2 Lentiviral Packaging Plasmid – Addgene, UK

Puromycin – InvivoGen, USA

RNAGEM Tissue Plus Kit – ZyGEM, New Zealand

Saponin – Donated By Dearden Lab, University Of Otago, NZ

Sodium Chloride – Scharlau, Spain

Sodium Pyruvate – Invitrogen, USA

Trypan Blue – Sigma-Aldrich, USA

Tryptone – Scharlau, Spain

Ultra-Pure Distilled Water – Invitrogen, USA

Viraclean – Whiteley Medical, Australia

VSVG Lentiviral Envelope Plasmid – Addgene, UK

Wortmannin – Selleckchem, USA

Yeast Extract – Merck, Germany

2.1.2 EQUIPMENT

0.2mL Semi-Skirted 96-Well PCR Plate – Thermo Scientific, UK

0.2mM Hydrophilic Syringe Filter – Ahlstrom, Germany

0.22mM Polyethersulfone Vacuum Filter System – Jet Bio-Filtration, China

0.45mM Polyvinylidene fluoride Syringe Filter – Mereck, Ireland

0.6mL Microtube – Axygen, USA

1mL Syringe – BD, Singapore

1.5mL Microtube – Axygen, USA

10mL Serological Pipet – Jet Bio- Filtration, China

10mL Syringe – BD, Singapore

15mL Falcon Centrifuge Tubes – Greiner Bio-One, Germany

20mL Syringe – BD, USA

200mL Schott bottle – Schott North America, USA

25mL CELLSTAR Cell Culture Flasks – Greiner Bio-One, Germany

25mL Serological Pipet – Jet Bio-Filtration, China

384-Well Assay Plate 3707, White with Clear Bottom – Corning, USA

400mL Schott bottle – Schott North America, USA

50mL Falcon Centrifuge Tubes – Greiner Bio-One, Germany

75mL CELLSTAR Cell Culture Flasks – Greiner Bio-One, Germany

96-Well Assay Plate 3603 – Corning, USA

94mm × 16mm, vented disposable petri dish with lid – Brand®, Germany

ABI Prism 7900 HT – Applied Biosystems, USA

C1000™ ThermoCycler – Bio-Rad, USA

Cell Culture Dishes 100x20mm – Greiner Bio-One, Germany

Centra 3c Centrifuge – International Equipment Company, UK

Centrifuge 5810 – Eppendorf, Germany

CO_2 Cell Culture Incubator – Binder, Germany

Cryo Vials – Nunc, Denmark

Cytation 5 Cell Imaging Multimode Reader – BioTek, USA

Cytell Cell Imaging System – GE Lifesciences, USA

Double-Chambered Cell-Counting Slide – Bio-Rad, USA

IEC Centra-3C Centrifuge – International Equipment Company, USA

IncuCyte ZOOM System – Essen Bioscience, USA

Inoculating Loops – Nunc, Denmark

Magnetic Stirrer MR 001 – Heidolph, Germany

Microamp Optical 384-Well Reaction Plate – Life Technologies, USA

Milli-Q Ultrapure Water Purification System – Millipore, USA

NanoDrop ND-1000 Spectrophotometer – NanoDrop Technologies, USA

NucleoBond Xtra Midi Plasmid DNA purification – Macherey-Nagel, Germany

NucleoSpin Plasmid DNA purification – Macherey-Nagel, Germany

Olympus CK2 Microscope – Olympus, Japan

Pasteur Pipettes – Hirschmann, Germany

Solution Basin – Biologix, Group

TC10 Automated Cell Counter – Bio-Rad, USA

Thermal Seal, Real-Time PCR Optical Plastic Sheet – Interlab Ltd, NZ

Tissue Culture Hood – EMAIL, Australia

Water Bath – Semco, USA

2.2 CELL CULTURE

2.2.1 293FT CELLS

293FT cells were used for the production of the shRNA lentivirus as their SV40 large T antigen allows for high protein expression. They are derived from 293F human embryonic kidney cells and provide a high lentiviral titre.

2.2.1.1 293FT CELL MEDIA

The following components were filtered through a 500mL 0.22μm Polyethersulfone (PES) Vacuum Bottle Filter (Jet Bio-Filtration): DMEM, FBS, L-Glutamine, Sodium pyruvate and Non-essential AA (Table 3).

Table 3 - Constituents of the 293FT media.

Constituents	Concentration
DMEM (500mL)	88%
FBS (50mL)	8.8%
L-Glutamine (5mL)	6mM
Sodium pyruvate (5mL)	1mM
Non-essential AA (5mL)	0.1mM

2.2.1.2 293FT CELL RECOVERY

293FT cells stored in liquid Nitrogen at a low passage stock (12 – 13) were removed and warmed in a 37°C water bath. When defrosted they were added to a T25 flask with fresh warmed media. Cells were passaged the following day to a T75 flask.

2.2.1.3 PASSAGING 293FT CELLS

293FT cells are very sensitive and therefore must be handled with utmost care, as rough handling will dislodge the cells. Complete confluence was avoided as the cells began to peel away and form sheets. To passage, cells were incubated in phosphate buffer saline (PBS) with 0.05% trypsin at room temperature for 5min. Fresh media was then added to wash off cells and transfer to a 15mL falcon. Cells were spun at 500rpm for 5 min to pellet. Supernatant was aspirated and the pellet was resuspended in 5mL media. $1x10^6$ cells were seeded in a T75 flask or 10cm cell culture to reach 90% confluence in 4 days.

2.2.2 MCF10A CELLS

MCF10A cells and their isogenic partner *CDH1*$^{-/-}$ (Sigma-Aldrich) were used to model non-tumourgenic epithelial cells for this study. MCF10A cells are diploid and dependent on exogenous growth factors to proliferate and are considered a normal epithelial cell model. Coming from breast tissue, MCF10A are biologically relevant as HDGC predisposes female *CDH1* germ line mutation carriers to LBC.

2.2.2.1 MCF10A CELL MEDIA

The following components were filtered through a 500mL 0.22μm Polyethersulfone (PES) Vacuum Bottle Filter (Jet Bio-Filtration) (Table 4).

Table 4 - Constituents of the MCF10A media.

Constituents	Concentration
DMEM/F12 (500mL)	95%
Horse Serum (25mL)	5%
Insulin (1.4mL)	(10μg/mL)
Hydrocortisone (250μL)	(0.5μg/mL)
EGF (100μL)	(20ng/mL)

2.2.2.2 MCF10A CELL RECOVERY

MCF10A and *CDH*$^{-/-}$ cells were stored in liquid nitrogen at a passage of 4-5. They were warmed in the 37°C water bath before being added to 10mL of MCF10A media in a 15mL tube. The 15mL falcon was centrifuged at 900rpm and the supernatant discarded. Cells were resuspended in complete MCF10A media and were all added to a T25 cell culture flask. After 24 hrs the morphology confirmed the difference between the MCF10A and *CDH*$^{-/-}$ cell lines as MCF10A grow faster and are less clumped. Cells are thereafter passaged every 3-4 days before reaching confluence.

2.2.2.3 PASSAGING MCF10A CELLS

To passage the MCF10A and *CDH*$^{-/-}$ cells, they were rinsed in PBS before leaving for 20 minutes (min) at 37°C in 0.05% trypsin to lift the cells. Media was added to wash the cells off the plate and the cells were moved to a 15mL tube. The tubes were centrifuged at 800rpm for 5 min and the supernatant discarded. Fresh 37°C media was added to resuspend the pellet and the cell density counted using the double-chambered cell counting slide in the TC10 automated cell counter (Bio-Rad). The MCF10A cells were seeded at 4000 cells/cm^2 in either a T25 or T75 flask and *CDH1*$^{-/-}$ cells were seeded at 6000cells/cm^2, as they took longer to grow. Cells were incubated at 37°C for four days at which they would reach 90% confluence.

2.3 CREATING THE SHRNA LENTIVIRUS

The shRNA (Dharmacon) are packaged in a GIPZ plasmid and supplied in *Escherichia coli* (*E.coli*). The GIPZ plasmid contains GFP for confirmation of the transduction. It also contains ampicillin and puromycin resistance genes that help isolate and select for the cells or *E.coli* which contain the plasmid. The plasmids were packaged in 293FT cells, and a titre was calculated in MCF10A cells.

2.3.1 PLASMID PREPARATION

The following GIPZ plasmids contained in individual *E.coli* colonies were used in these experiments: 10 shRNA with individual *PLK3* and Non-silencing, targeting sequences (Table 5 and **Figure 9**), vesicular stomatitis

viral glycoprotein (VSVG) and the second-generation packaging vector (psPAX2). Glycerol stocks of the *E.coli* were stored at -80°C and using an inoculating loop they were streaked on separate lysogeny broth and agar plates with 100μg/mL ampicillin for each specific shRNA (Chapter 5.1 for Lysogeny broth agar plates and 5.2 for Lysogeny broth components). Ampicillin was used to select for *E.coli* containing the plasmid. Plates were incubated overnight at 37°C. The following day only a single colony from each plate was inoculated to a separate tube with 15mL lysogeny broth and 100μg/mL ampicillin solution and was shaken overnight at 37°C.

Table 5 - shRNA sequences. The shRNA used in these experiments named after the well they originated from, their target gene and the sequence that targets that gene.

Origin	Target	Sequence of shRNA
E4	PLK3	AGTGAACCTGCTTGATGCA
E5	PLK3	AGTGCACAGTCTTTCTGTT
E6	PLK3	TGAAGAGCACAGCCACACG
E7	PLK3	ACTCTTCTTCTTTCTGCCA
E8	PLK3	TGTAGTGCACAGTCTTTCT
E9	PLK3	AGCTGGGAGCTAAGGCTCA
E10	PLK3	TTAGGATCTTCTCGCGCTG
E11	PLK3	TCAGGTGCTGTCTCTACCA
E12	PLK3	TTTCTCAGAGCACAAAGGG
F1	PLK3	AGTGGTCCATAAATAACGC
Non-Silencing	-	CTTACTCTCGCCCAAGCGAGAG

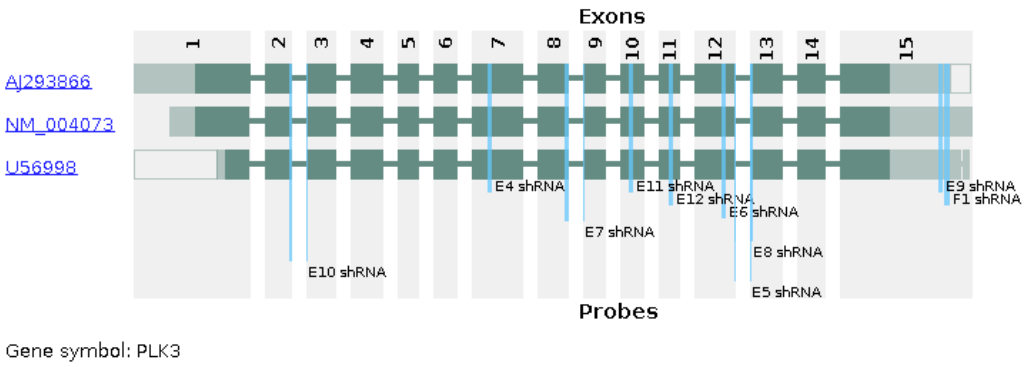

Figure 9 - shRNA sequences targeting the *CDH1*$^{-/-}$ gene. The transcript of CDH1 displayed with the exons as green blocks and introns as the connecting lines. The vertical blue lines indicate the sequences of shRNA (labelled by their identifier) that match on this gene. This was performed using an online tool "siRNA check" developed by Silico Solutions.

To obtain a high quantity of the VSVG and psPAX2 plasmids, the spin column based NucleoBond Xtra Midi Prep kit (Macherey-Nagel) was used to separate the plasmids from the *E.coli*. For the *PLK3* shRNA, the NucleoSpin plasmid DNA purification kit (MACHEREY-NAGEL) spin column protocol was used.

The amplified *E.coli* in the lysogeny broth and ampicillin culture was centrifuged to form a pellet and the supernatant discarded. The NucleoSpin plasmid DNA purification protocol was then followed except after resuspending the pellet; two 200µL aliquots of the suspended pellet in buffer were extracted. Each shRNA plasmid then had two quantities that proceeded through the protocol, which increased the quantity.

To elute the plasmid DNA out of the spin column, the elution buffer was left to incubate for 15 min rather than just one as previous optimisation found this yielded greater quantity. Centrifuging the column and repeating the elution was gave a greater plasmid yield. This was repeated with the two

aliquots from each *E.coli*, producing two quantities with a final volume of 110μL. The two volumes were combined giving a greater final quantity.

2.3.2 TRANSFECTION

In order to produce an shRNA lentivirus, the shRNA, a packaging vector psPAX2 and an envelope vector VSVG were transfected into 293FT cells to package the pGIPZ shRNA plasmid. $5.4x10^6$ 293FT cells were seeded in a T75 cell culture flask in 293FT media 24 hrs before transfecting the plasmids. The following day, the concentration of extracted plasmids (Chapter 2.3.1) was measured using the NanoDrop ND-1000 Spectrophotometer to determine the volume required to add 18.56μg shRNA plasmid, 9.6μg psPAX2 and 4.8μg VSVG to each transfection. These were mixed in 1mL of filtered Opti-MEM solution, a media derived from Eagle's Minimum Essential Media that aids transfection, due an increased amount of HEPES buffer that aids the transfection. Separately, 55.7μL Lipofectamine 2000 was added to 944.2μL of Opti-MEM, in a separate tube for each shRNA lentivirus to be created. The 1mL solution containing the shRNA, psPAX2 and VSVG was filtered through a 0.22μm hydrophilic filter into the 1mL lipofectamine and Opti-MEM mix and incubated at room temperature for 20 min. This allowed for the liposome to encase the plasmids that aids uptake by helping the vessels cross the cell membrane. The media was removed from the 293FT cells and were washed in PBS. Opti-MEM with 5% foetal bovine serum (FBS) was added, along with the

liposomes containing the shRNA, psPAX2, VSVG. Plates were returned to the 37°C incubator.

After a further 24 hrs, media was removed from the flask followed by a gentle PBS wash. This was replaced with 6mL complete 293FT cell media. At 48 hrs post transfection, the 6mL of media from the 293FT cells was collected and centrifuged for 15 min at 3000rpm. The supernatant containing the lentivirus was filtered through a 0.45μM Polyvinylidene fluoride filter and aliquoted into 10 lots of 500μL to be stored at -80°C. Each 500μL was used only once to remove any effects of repeated thawing and freezing.

2.3.3 TITRE

A titration determines the amount of viral transducing units (TU) contained in the harvested virus. The titre was determined by measuring the quantity of MCF10A cells expressing the GFP reporter from the shRNA plasmid. A serial dilution created a range of concentrations that the amount of TU/mL was derived from. At low concentrations of virus, for every GFP positive cell, there is only one transducing unit for that cell. At higher concentration, multiple transducing units/cell may occur, which would skew the count of TU/mL.

MCF10A cells were seeded at $4x10^4$cells/well in 100μL into a 96 well plate with black walls and a clear bottom compatible with fluorescent imaging. After 24 hrs, the lentivirus (Chapter 2.3) was diluted by a factor of 2 five times to provide a range of six concentrations (**Figure 10**). 100μL of each

dilution was added to the cells in their 100μL of media creating a further 2 fold dilution to have a final dilution range of 1:1, 1:3, 1:7, 1:15, 1:31, 1:63. A additional well of 100μL media only served as a negative control.

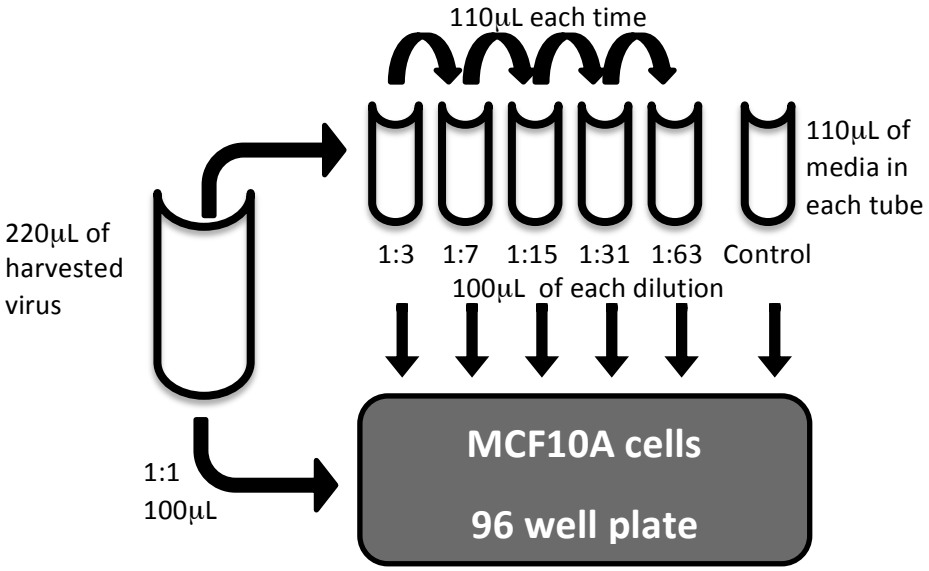

Figure 10 - Lentivirus dilution for titre. Harvested lentivirus was diluted and added to the 96 well plate.

After 24 hrs, media was aspirated and 100μL of warmed MCF10A media was added. After a further 24 hrs the plates were imaged using the Automated Imaging BioApp on the Cytell Cell Imaging System (GE Lifesciences). 10 fields at 10x magnification in the GFP channel were captured for each well. GFP expression confirms that the cell has incorporated the shRNA into its genome and was expressing the shRNA plasmid genes.

The images of either the 1:63 or the 1:31 final dilution were used to count the GFP expressing cells as this range had 50% of the cells expressing GFP, which corresponds to only one transducing units/cell. Using the FIJI cell

imaging software program's cell counter plug-in (National Institute of Health) the quantity of cells expressing GFP were counted [70]. To cause a sufficient gene knockdown of *PLK3* in MCF10A cells, a multiplicity of infection (MOI) of 15 was required, meaning 15 transducing units/seeded cell, as previously determined in the lab by Tom Brew and James Frick.

The average count from the 10 fields was calculated and multiplied by 54.494 to determine the TU/mL that was in the diluted 100μL. The transducing units/well was multiplied by the dilution and multiplied by 10 to convert to TU/mL. The 15 transducing units/seeded cell required 15,000 transducing units in 50μL and was calculated using the density of the seeded cells.

2.4 TRANSDUCTION

To test the synthetic lethal effect of a genetic knockdown of *PLK3*, the shRNA created in Chapter 2.3 were transduced into MCF10A and *CDH1*$^{-/-}$ cells. Their viability was measured by cell counting and the knockdown was measured by RT-qPCR.

2.4.1 CELL VIABILITY

1x10^{4}cells/well of MCF10A and 1.5x10^{4}cells/well of *CDH1*$^{-/-}$ cells were seeded in a 96 well plate in 100μL of media and incubated at 37°C. *CDH1*$^{-/-}$ cells were seeded at a higher density to reach confluence at 72 hrs as it was previously determined they take longer to adhere will have a parallel growth rate to MCF10A cells. After 24 hrs the shRNA lentivirus was

defrosted at room temperature and diluted in media. 50μL of the lentivirus containing 15 transducing units/seeded cell, was added to the 100μL of media and cells in appropriate wells. 1-3 shRNA were tested each time, in addition to cell only, non-silencing and no insert controls. The non-silencing no insert and cell only acts as control to normalise any non-specific effects of shRNA transduction.

The cells on the outer wells were always excluded due to edge effects and instead these wells were stained with 1μg/mL of Hoechst 33342 at 24 hrs as a quality control measure. Using the Cytell, stained cells were imaged at 4x magnification with four fields in the phase and DAPI channels. Images were counted on Cell Profiler selecting the nuclei for each cell. Cell Profiler is a software that allows large image sets to be processed over a wide range of variable parameters that are able to specifically identify and count cells [71]. Counts were analysed to confirm that the plates were seeded evenly. Plates with uneven seeding density were discontinued before introducing the lentivirus. Once treated, cells were kept at 37°C and 5% CO_2 and handled in accordance with viral containment conditions.

At 24 hrs post transduction, the media was changed by aspirating all 150μL from the wells and adding 100μL of fresh complete MCF10A media with 1μg/mL puromycin. Puromycin selected for transduced cells as the pGIPZ shRNA contained puromycin resistance. This was not be added to the cell only wells as they do not express any resistance. Any cells not transduce would die as a result of the puromycin. All remaining cells express shRNA causing the knockdown of *PLK3*. This selection allowed the total cell count

to accurately portray the differential effect on cell viability with and without *PLK3*.

At 72 hrs post transduction all media was removed from the wells. Two wells from each treatment group were used for RNA extraction (Chapter 2.4.2). The remaining wells were stained with 1μg/mL of Hoechst 33342 and 0.5ug/mL propidium iodide in PBS for a minimum of half an hour and imaged using the Cytell. Images from four fields at 4x magnification were taken using the Cytell's Automated Imaging BioApp, or quantified came directly by counting the cells from 20 fields at 10x magnification using the Viability or Cell Cycle BioApp. As a quality control Cell Profiler used the 4x images to also count the amount of cells [71]. Results were analysed by calculating the sum of the nuclei in each well. Technical replicates were averaged for total cell count response to treatment. *PLK3* knockdown samples were normalised to the non-silencing treatment for each cell line, to compare responses to treatment.

2.4.2 RNA EXTRACTION AND REVERSE TRANSCRIPTION

72 hrs after transduction, two wells from each cell line treatment group were examined to validate the knockdown efficiency using RT-qPCR. Wells were washed with PBS, and the *RNA*GEM Tissue PLUS kit (ZyGem) was used. The amount of cells per well was ~5000 and therefore a master mix with of 12.5μL of *RNA*GEM enzyme, 62.5μL of SILVER buffer and 925μL of MQ H_2O 25μL mix was required. 25μL of the mix was added to the 40 wells, dislodged with a pipette tip, transferred to a PCR strip tube and heated to

75°C in a ThermoCycler. This serves to activate the enzyme, ensures cell lysis and the removes of RNAses by protein lysis. A second step with DNAses in the ThermoCycler at 37°C for 5 min followed by 75°C for 5 min, removed any DNA from the RNA extract. TE-buffer was added so that the pH was stable, serving to protect the RNA from degradation.

Reverse transcriptase (RT) was used to synthesize cDNA from the purified RNA. The PrimeScript RT reagent Kit (TAKARA) was used to produce the cDNA following the 'SYBR Green assay protocol'. This involved creating 3.5μL/reaction of a combined buffer, RT enzyme, oligo dT Primer and Random 6 mers. 6.5μL of purified RNA was added to 3.5μL of the mix producing a final volume of 10μL/reaction, which was incubated in the ThermoCycler at 37°C for 15 min (reverse transcription) and 85°C for 5 sec (enzyme inactivation). Two negative controls were also included, one lacking the RT enzyme, the other lacking the template.

2.4.3 RT-qPCR

The KAPA SYBR FAST RT-qPCR Kit protocol (Kapa Biosystems) was used to carry out RT-qPCR of the cDNA and was the final process in determining whether *PLK3* was successfully knocked down.

Housekeeping genes *GAPDH* and *PPIA* were used to normalise *PLK3* expression. Primers were purchased from Integrated DNA Technologies *PLK3* was designed using Primer3 [72], *GAPDH* and *PPIA* were pre-designed (primer sequences in Appendix 5.3). A 1:6 dilution of the cDNA was used to negate any effects from residual reverse transcriptase. 5μL of

the cell only control cDNA from each cell line was used to create a series of five four-fold dilutions to calculate a standard curve and obtain the efficiency of the RT-qPCR reaction (**Figure 11**). This enabled the use of the Pfaffl method to analyse the results [73].

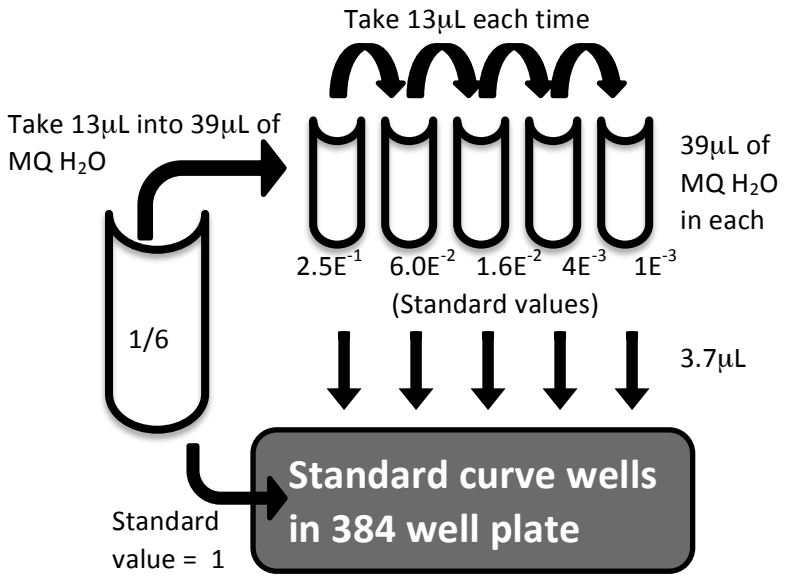

Figure 11 – The 1:4 dilutions carried out for the standard curve of the RT-qPCR

Each sample was performed in duplicate in an 8µL reaction. The 8µL consists of 3.7µL of the 1:6 dilution of template cDNA, 4µL of 2xKAPA SYBR FAST RT-qPCR mix, 0.12µL of forward and reverse primers (300nM), 0.16µL of 50X ROX reference dye to normalise the signal, and 0.02µL of MQ H_2O. This was carried out on a 384-well assay plate to accommodate for the 180 reactions per experiment including negative no template controls of MQ H_2O. The RT-qPCR was run in the ABI Prism 7900HT with an enzyme activation step of 95°C for 3 min followed by 40 repeats of denaturation 95°C for 15 sec, annealing at 57°C for 15 sec, and data acquisition at 72°C for 15 sec. The dissociation stage of 95°C for 15 sec and 60°C for 15 sec

provided the final dissociation step and gave a melt curve to distinguish the products of the reaction.

2.4.4 GEL AND SEQUENCE

To validate the RT-qPCR primers and ensure we were testing the right sequence, one of the products of the *PLK3* RT-qPCR was analysed on a 1.5% agarose gel electrophoresis and another was also sent to University of Otago DNA sequencing service.

The 1.5% agarose gel was made using 1x ethydium bromide and Tris base, acetic acid and EDTA buffer solution. 0.75g of agarose was added to 50mL of the buffer and microwaved till clear. The solution was poured into a gel electrophoresis cast (LABREPCO) and left to set. The buffer was poured around the gel and product was mixed in a 4-fold dilution with 2x bromophenol blue dye and loaded into the gels well alongside the Kapa Universal ladder. The gel was run for 30 min at 95 volts. Images were taken using the ChemiDoc MP System (Bio-Rad).

To prepare for sequencing the potential 93bp RT-qPCR *PLK3* product, was taken from the cell only well, as expression was higher in this treatment. The product was cleaned up in a spin column by adding ethanol (EtOH) and Sodium Acetate (NaAc) and washed out with 40°C H_2O. 1µL of either the forward or reverse *PLK3* primers was added to 1µL of the cleaned RT-qPCR product and diluted with 3µL of MQ H_2O for each primer, according to the Otago Genetic Analysis Sequencing Reaction Protocol. The results from

their sequencing were analysed using SeqMonk (Babraham Bioinformatics).

2.5 POLOXIPAN AND WORTMANNIN

To determine if current PLK3 inhibitors caused synthetic lethality we used poloxipan (Vitas-M Laboratory) and wortmannin (Selleckchem) at a range of concentrations to detect viability changes in MCF10A and *CDH1*$^{-/-}$ cells. These inhibitors were diluted until soluble in a stock solution of DMSO. 96-well black walled, clear bottom plates were seeded with $4x10^4$/well MCF10A and *CDH1*$^{-/-}$ cells and incubated at 37°C in an IncuCyte (Essen Bioscience). The IncuCyte takes phase contrast images of three fields/well at 4x magnification every two hrs. Inbuilt software determines the cell confluence over time, which correlates to their proliferation rate.

At 24 hrs, 11μL of the PLK3 protein inhibitor was applied to the cells from a range of two fold dilutions in MCF10A complete media (controls equivalent to the concentration of DMSO in the highest dosage of the inhibitor were included). Poloxipan was optimized to range from final concentrations of 0.25μM – 4μM. Wortmannin was optimised to range from 0.625μM – 10μM. After treatment the plates were returned to the IncuCyte for a further 48 hrs.

48 hrs post treatment the cells were stained with 1μg/mL Hoechst 33342 and 0.5μg/mL propidium iodide and imaged on the Cytell or the Cytation Cell Imaging Multimode Reader (BioTek). The same parameters were used

in imaging the shRNA treatments nuclei on the Cytell BioApps (Chapter 2.4.1). Hoechst nuclei staining and imaging from the Cytation gave an accurate total cell count from fluorescent imaging of six fields at 4x magnification. Cell count was confirmed by analysing the same images on Cell Profiler. Comparing the treatments after normalising to the DMSO controls for each cell line formed the difference in viability between various concentrations of the inhibitor between each cell line.

3 RESULTS

"Somewhere, something incredible is waiting to be known." – Carl Sagan

The recent genome-wide siRNA screen conducted in our lab identified *PLK3* as a putative synthetic lethal candidate of *CDH1*$^{-/-}$ cells [27]. This screen observed that *PLK3* knockdown caused a significant yet selective inhibition to growth in *CDH1*$^{-/-}$ cells compared to MCF10A cells. The screen resulted in a viability ratio of 0.84 calculated from the *CDH1*$^{-/-}$ cells having a viability of 76% compared to a viability of 90% in the MCF10A cells. The aim in this study was to validate the synthetic lethal interaction between *CDH1*$^{-/-}$ and *PLK3*, to provide further evidence of *PLK3* as a potential target for HDGC preventative treatment. This was achieved by knocking down the expression of *PLK3* mRNA using shRNA and using PLK3 inhibitors poloxipan and wortmannin.

In the shRNA knockdown of *PLK3*, two shRNA were successful. A synthetic lethal trend was observed in one and not in the other. The synthetic lethal relationship was not greater than the viability ratio threshold of 0.85 set at the siRNA high throughput screen. The p-values distinguishing the difference between MCF10A and *CDH1*$^{-/-}$ after *PLK3* knockdown from both shRNA were not significant. The treatment of poloxipan and wortmannin targeting PLK3 did not reveal a significant synthetic lethal phenotype. This indicates that *PLK3* and *CDH1* do not have a true significant lethal relationship.

3.1 *PLK3* SHRNA

Seven different shRNA plasmids (Dharmacon) targeting *PLK3* were used for the knockdown experiments. The shRNA plasmids were propagated in overnight cultures, extracted and quantified before viral packaging. The shRNA plasmids were transfected alongside psPAX2 and VSVG in 293FT cells to produce the *PLK3* targeting virus (Chapter 2.3). A viral titre determined if there is subsequent quantity of virus to proceed with transduction and RT-qPCR determined whether the viability reflects a true knockdown of *PLK3*.

3.1.1 VIRAL TITRE YIELD

The required viral titre needed to exceed $4.5x10^5$ TU/mL in order to achieve a MOI of 15 viral particles/seeded cell. All transfections produced sufficient concentrations except for the shRNA identified as E12 and this was not used for transductions (Table 6).

Table 6 - The titre of the shRNA and the number of transductions that were conducted from each virus.

shRNA ID	Target	Titre (TU/mL)	The Number of Transductions Conducted
E4	PLK3	$5.9x10^5$	5
E5	PLK3	$7.9x10^5$	2
E6	PLK3	$7.4x10^5$	1
E7	PLK3	$8.3x10^5$, $1.5x10^6$	9
E11	PLK3	$5.4x10^5$	5
E12	PLK3	$1.7x10^5$	0
F1	PLK3	$4.9x10^5$	4
NS	-	$1.1x10^6$	Control (used in all)
NI	-	$2.98x10^6$	Control (used in all)

3.1.2 POST TRANSDUCTION VIABILITY

MCF10A and *CDH1*$^{-/-}$ cells were seeded in a 96 well plate and transduced with one of the six shRNA viruses. Included in every biological repeat were cell only, no insert shRNA and non-silencing shRNA controls. Puromycin selected for the cells that were transduced by the virus. After 72 hrs post transduction of the virus, cells were stained and imaged In the Cytell. This provided a total cell count in each well with 4 technical repeats for each treatment. Viability of the treatment was determined by normalising each treatments average total cell count to the equivalent average total cell count of the non-silencing control for each cell line. A normalised value of 1 correlates to no effect, if the normalised viability was <1 it was lethal. If >1 the treatment promoted growth and was not lethal. Viabilities from MCF10A and *CDH1*$^{-/-}$ cells were compared to calculate the viability ratio which is considered synthetic lethal if ≥0.85.

26 knockdowns were conducted using the six different shRNA sequences (Table 6). From the 26 knockdowns, ten were excluded due to suboptimal consistency in seeding density leaving the results of only four shRNA. Primary results trended towards a synthetic lethal response due to decreased viability in *CDH1*$^{-/-}$ cells compared to MCF10A cells. Each individual shRNA had variable viability responses between the cell lines as the viability ratio was not always synthetic lethal (Table 7 and

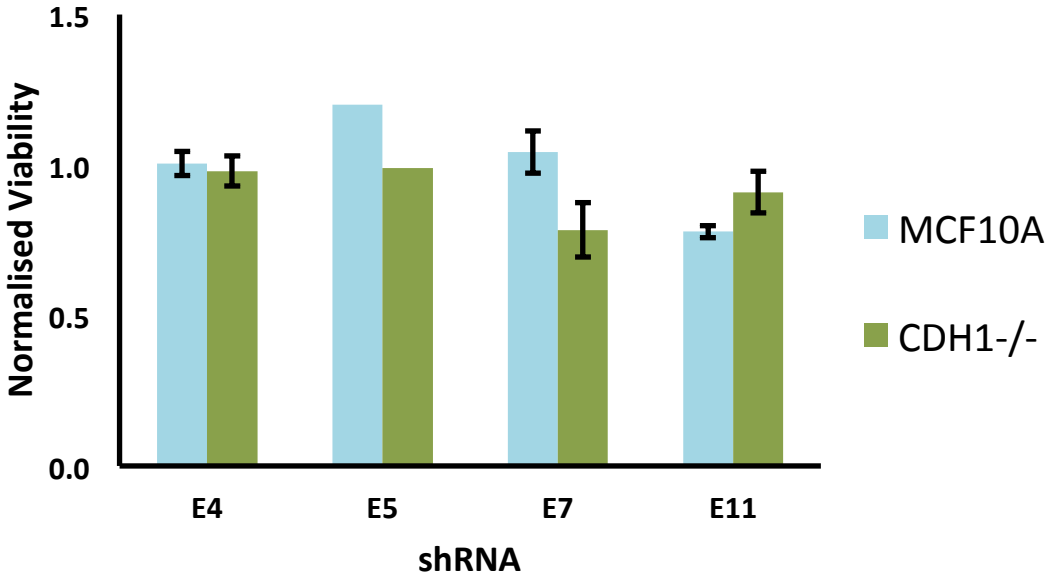

Figure 12). The greatest synthetic lethal response was seen in response to the knockdown from shRNA E7 (n=7) with a viability ratio of 0.75. The E11 shRNA treatment (n=3) did not produce a synthetic lethal response. E5 had one biological repeat which was synthetic lethal, and E4 had no effect considering the insignificant p-value. To validate the true relationship between *PLK3* and *CDH1,* the *PLK3* knockdown needed confirmation by determining the expression level of *PLK3* derived from RT-qPCR.

Table 7 - Average effect of the attempted *PLK3* shRNA knockdown on MCF10A and *CDH1*$^{-/-}$ cell viability.

shRNA	MCF10A Viability	*CDH1*$^{-/-}$ Viability	Viability Ratio	P-Value
E4	1.01	0.98	0.98	0.72
E5	1.20	0.99	0.82	-
E7	1.04	0.78	0.75	0.08
E11	0.78	0.91	1.17	0.22

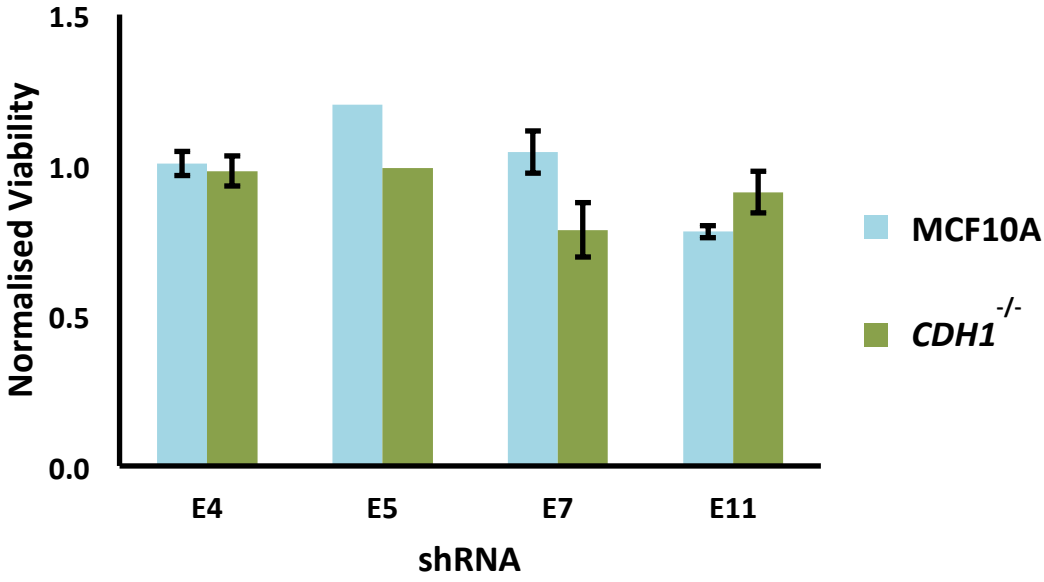

Figure 12 – Average of the normalised viability of MCF10A and *CDH1*$^{-/-}$ cells after shRNA treatment. Cells were transduced with shRNA, stained and imaged to determine a total cell count. Viability was determined by normalising the total cell count to the non-silencing control. E4 n=5, E5 n=1, E7 n=8 and E11 n=2.

3.1.3 P*LK3* KNOCKDOWN EFFICIENCY.

The cell viability study needed confirmation that *PLK3* had been knocked down by the lentiviral constructs. The expression of *PLK3* was analysed using the Pfaffl method [73]. The Pfaffl method uses the efficiency of the reaction derived from the slope of the standard, in an equation with the cycle threshold (Ct) of the control and the Ct of the sample/treatment the expression is being calculated for. This value from the *PLK3* knockdown is normalised to the average of the values of the two housekeeping genes *GAPDH* and *PPIA.* Two technical repeats of each genes expression from the *PLK3* knockdown are averaged and normalised to the non-silencing controls within that cell line.

To confirm that the RT-qPCR was actually measuring the expression of the *PLK3*, *GAPDH*, and *PPIA*, the products of the reaction were ran on a gel and sent for sequencing. The RT-qPCR products were separated by size through electrophoresis on a 1.2% agarose gel. In comparison with the Kapa Universal ladder the size of the *PLK3* product was around 100bp. This indicated that our product from the RT-qPCR was *PLK3* as the primers were designed to produce a 93bp product. *PPIA* primers produced the expected 138bp product but it also very small amounts of a 450bp product. The larger product is indicative of contamination. The *GAPDH* primers produced a band at the expected size of 200bp (**Figure 13**).

The PLK3 product was also confirmed by sequencing the reactions product. To prepare the RT-qPCR *PLK3* product for sequencing, the product was cleaned in a ethanol spin column wash and diluted in MQ H_2O with either

the forward or revers primer it was sequenced with. The sequences of both the forward and reverse reactions was a match with the expected sequence in the *PLK3* gene. This confirmed that the RT-qPCR was testing for *PLK3* expression.

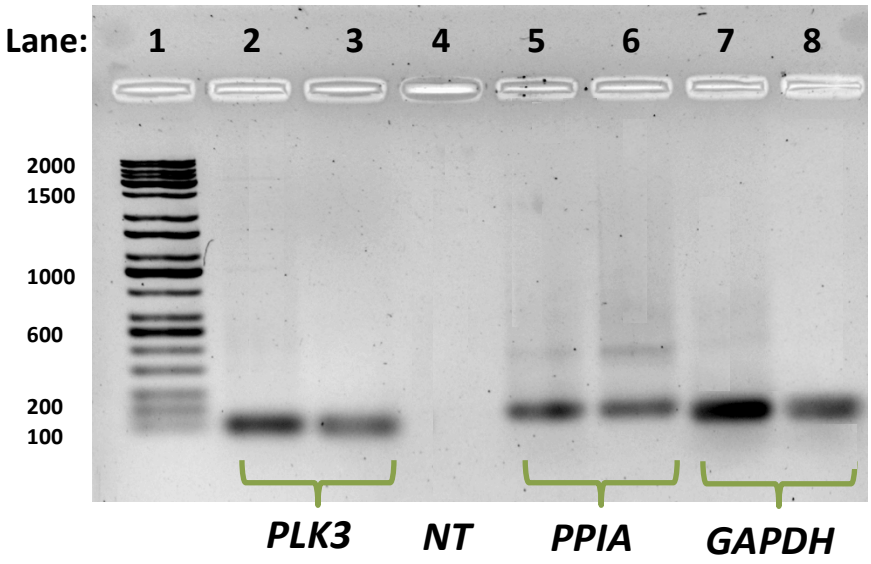

Figure 13 - Agarose gel containing the products of the RT-qPCR reaction. Lanes are as follows: 1 = ladder, 2 = *PLK3* from cell only (CO) control, 3 = *PLK3* from E4 shRNA treatment (E4), 4 = no template (NT) H_2O control, 5 = *PPIA* from CO 6 = *PPIA* from E4, 7 = *GAPDH* from CO. 8 = *GAPDH* from E$ All products were from MCF10A cells.

The expression of *PLK3* from the non-silencing controls did not undergo any knockdown and were considered as having normal expression. A normalised value of 1 correlated to no knockdown, >1 would mean the treatment had more *PLK3* than the control and <1 would mean there was less *PLK3*. A knockdown was considered successful if the level of *PLK3* was <0.5 (**Figure 14**).

There were five transductions that were successful in knocking down *PLK3* expression in both cell lines at the same time. Two were from E4, one from

E5 and three from E7. The 11 remaining transductions were only successful in knocking down *PLK3* in one or neither of the MCF10A or *CDH1*$^{-/-}$ cell lines. All repeats of E11 shRNA were unsuccessful in knocking down *PLK3* expression in both. These 11 unsuccessful knockdowns were withdrawn from comparison (**Figure 15**).

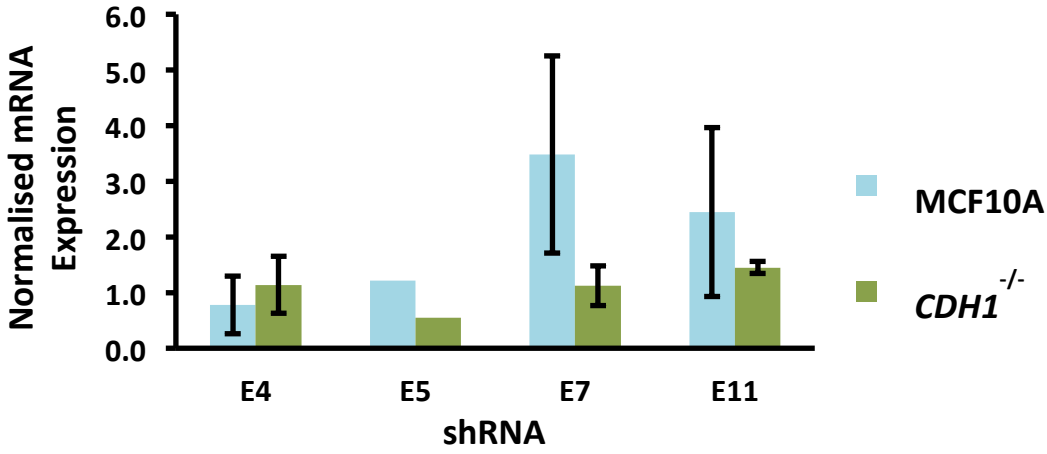

Figure 14 – Average of the normalised expression of PLK3 in MCF10A and *CDH1*$^{-/-}$ cells from <u>every</u> transduction. Values were normalised to the non-silencing control. A normalised value <0.5 is a successful knockdown as it means the expression was halved. The amount of biological repeats were: E4 n=5, E5 n=1, E7 n=8 and E11 n=2.

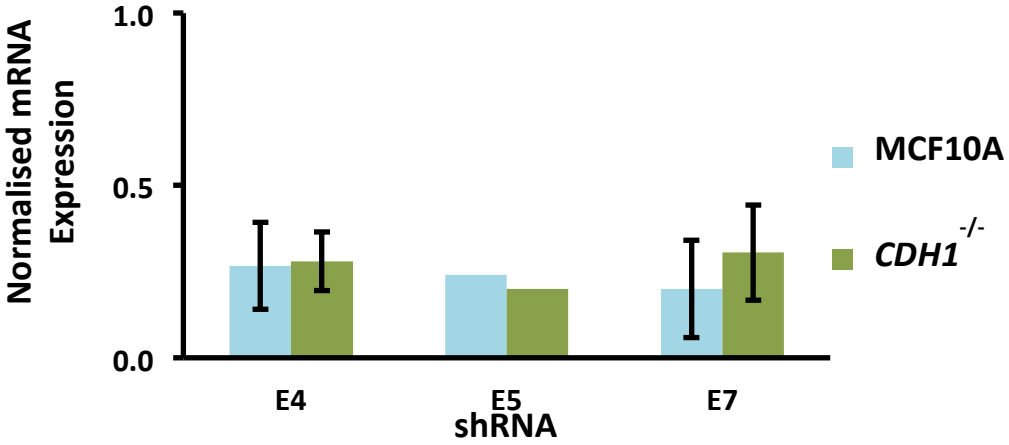

Figure 15 - Average of the normalised expression of PLK3 in MCF10A and *CDH1*$^{-/-}$ cells for the <u>successful</u> knockdowns. The normalised value of *PLK3* expression <0.5 was the threshold to be considered a successful knockdown.

Expression values were normalised to the non-silencing control. The amount of biological repeats were: E4 n=2, E5 n=1 and E7 n=3.

The average viability of a successful E4 *PLK3* knockdown did not meet the hypothesis because it caused a reverse synthetic lethal effect. The reverse synthetic lethal effect is a lower viability in the MCF10A cells compared to the *CDH1*$^{-/-}$ cells. A successful knockdown with E7 shRNA was consistent with the hypothesis as it shows a synthetic lethal effect (Table 8 and **Figure 16**). The p-value of both these results are not significant and therefore they indicate the null hypothesis should be accepted, meaning that there is no conclusive evidence of a either a synthetic lethal relationship or reverse synthetic lethal relationship between *PLK3* and *CDH1* (Table 1).

Table 8 - Viability of the MCF10A and *CDH1*$^{-/-}$ cells after successful PLK3 knockdown The viability is analysed with standard error (STD Error), p-value and viability ratio. A viability ratio ≤0.85 is considered synthetic lethal.

Viability of Successful *PLK3* Knockdowns						
shRNA	MCF10A		*CDH1*$^{-/-}$		Viability Ratio	P-Value
	Viability	STD Error	Viability	STD Error		
E4	0.69	0.26	1.14	0.17	1.65	0.18
E7	0.9	0.12	0.83	0.03	0.92	0.60

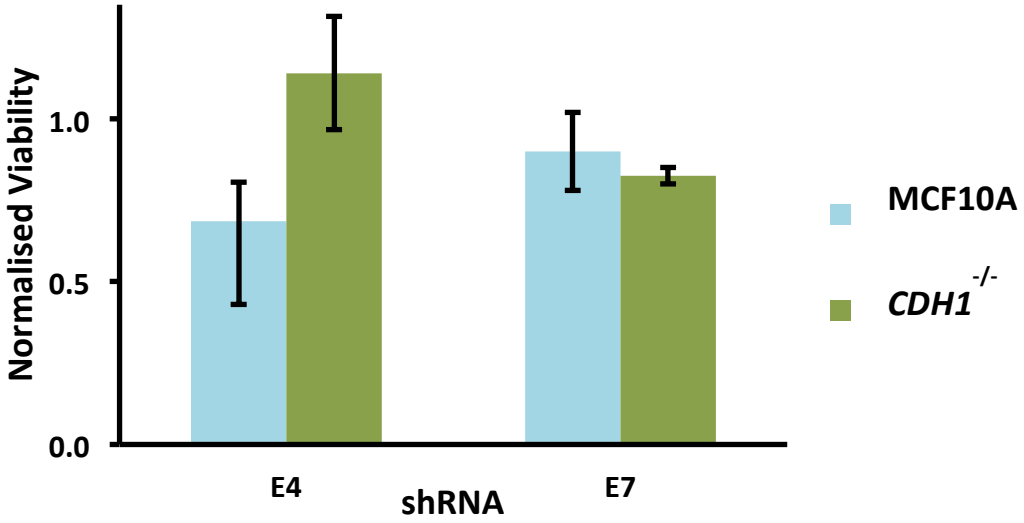

Figure 16 – Average of the normalised viability in MCF10A and *CDH1*$^{-/-}$ cells after successful PLK3 shRNA knockdowns. The amount of biological repeats were: E4 n=2 and E7 n=3. Dividing the average total cell count from the treatment by the average total cell count from the non-silencing control created normalised values.

3.2 POLOXIPAN

MCF10A and *CDH1*$^{-/-}$ cells were seeded in a 96 well plate and their confluence was imaged and measured using the IncuCyte. The images show the behaviour of the cells before and after treatment of poloxipan. Cells were treated with poloxipan 24 hrs after seeding, and stained and imaged to count the nuclei at 48 hrs. The total cell count provided determination of viability.

Poloxipan is a pan inhibitor of the polo-like kinase family. It is currently the most active PLK3 inhibitor with an IC_{50} of 3.0μM but it also inhibits PLK1 at 3.2μM. The concentrations we used were 0.25μM, 0.5μM, 1.0μM, 2.0μM, and 4.0μM.

3.2.1 GROWTH OF POLOXIPAN TREATED CELLS

The confluence from the IncuCyte showed that a range of concentrations of poloxipan did little to change the growth over time of the MCF10A cells (**Figure 17**)**.** The *CDH1*$^{-/-}$ cells responded to poloxipan treatment with a reduction of confluence after being treated. The *CDH1*$^{-/-}$ cells were able to recover and continue growing.

The images for the IncuCyte (**Figure 18**) show poloxipan would only stall the growth of MCF10A cells at the first 2 hrs, were as *CDH1*$^{-/-}$ cells actually regress. Any migrating *CDH1*$^{-/-}$ cells at the time of treatment retract and isolated cells associated together forming a tight rounded clumps. Images of the MCF10A cells showed little response to Poloxipan over the treatment period that indicates a high viability. In contrast, *CDH1*$^{-/-}$ cells clearly had growth inhibition. Quantifying the viability from the normalising the total cell count provided the further specification as to whether the treatment left the cells viable.

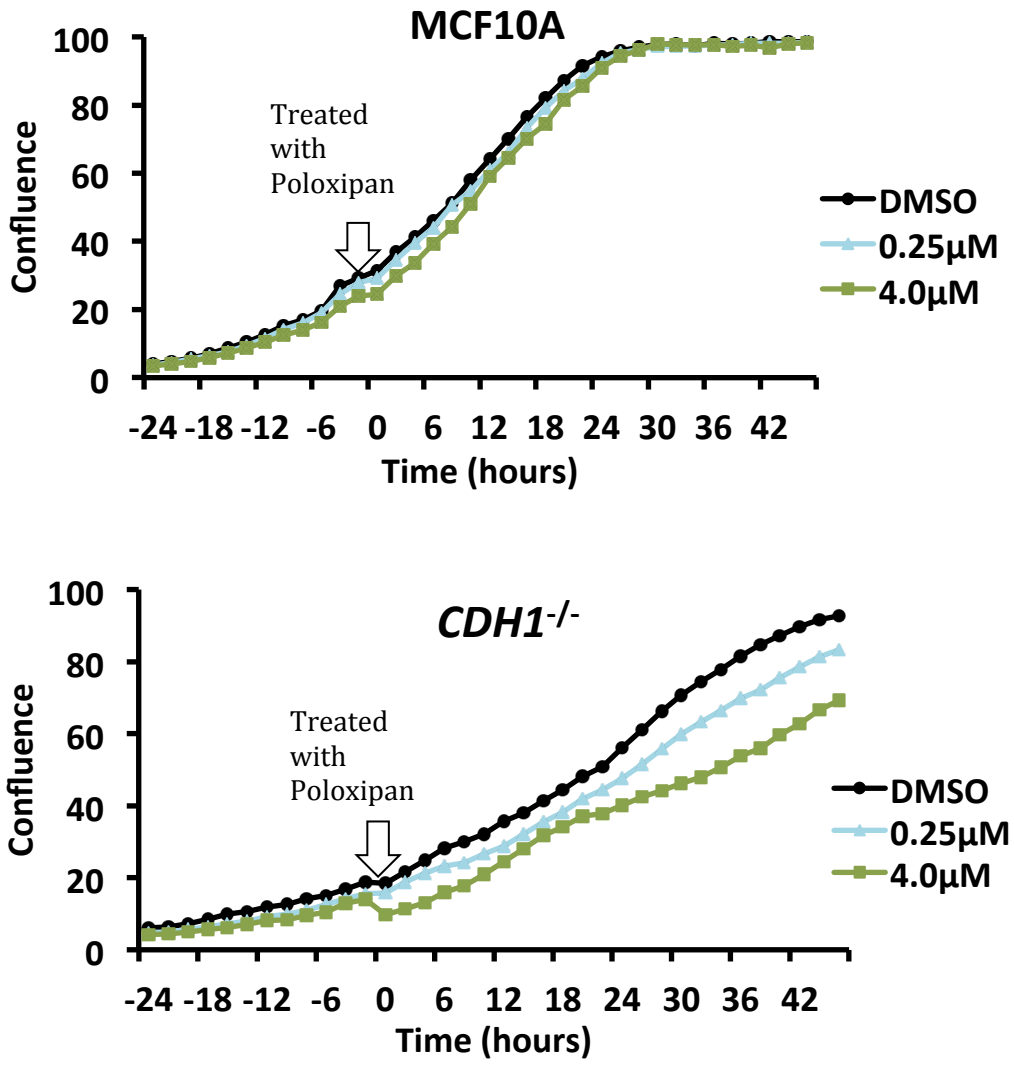

Figure 17 - Pre and post treatment confluence over time of MCF10A and *CDH1*$^{-/-}$ cells treated with 4µM of poloxipan Cells had from 3 technical repeats with confluence recorded every 2 hrs. Cells were treated with poloxipan after time 0 with a range of concentrations of which the lowest and highest (0.25µM and 0.4µM) are shown alongside the DMSO control.

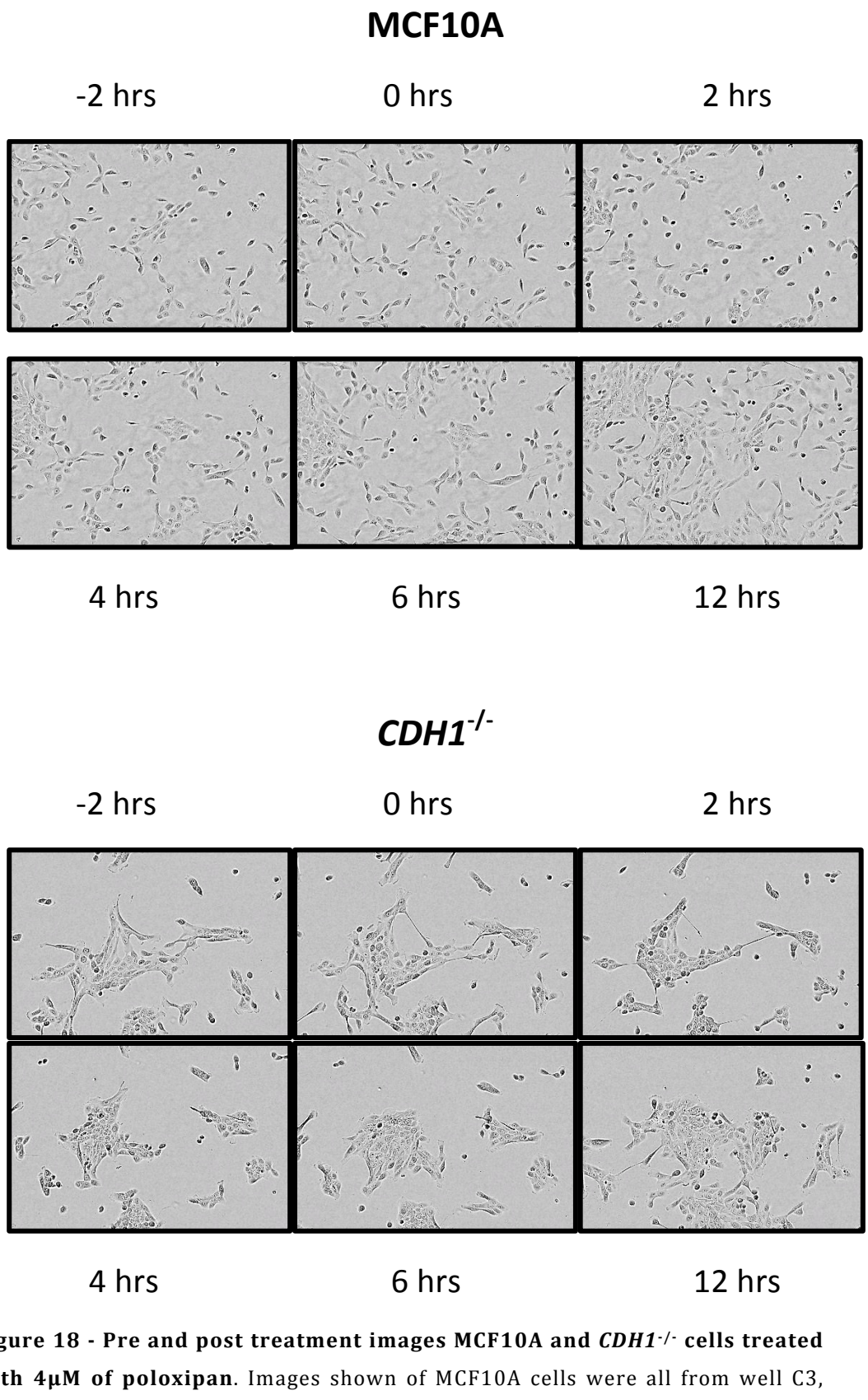

Figure 18 - Pre and post treatment images MCF10A and *CDH1*$^{-/-}$ cells treated with 4µM of poloxipan. Images shown of MCF10A cells were all from well C3, field 2; Images of *CDH1*$^{-/-}$ cells were all from well F3, field 3. Images were taken every 2 hrs, of which the -2, 0, 2, 4, 6, and 12-hour time points are shown. Treatment was administered after time 0. First response is seen at 2 hrs.

3.2.2 VIABILITY OF POLOXIPAN TREATED CELLS

The viability of four biological repeats gave conclusive results that PLK3 inhibition by poloxipan was not synthetic lethal to *CDH1*$^{-/-}$ cells. 48 hrs after poloxipan was administered the cell count was analysed by staining the cells, and analysed from the images taken using the Cytation and Cell Profiler. The cell count for each poloxipan treatment was normalised to the equivalent DMSO control of that cell type. The viability ratio was determined from the normalised viability of MCF10A and *CDH1*$^{-/-}$ cell lines (Table 9 and **Figure 19**). A treatment causing a viability ratio ≤0.85 is synthetic lethal, while a treatment causing a viability ratio >1 is having a reverse synthetic lethal effect. A reverse synthetic lethal treatment (when the MCF10A cells have a lower viability after treatment than the *CDH1*$^{-/-}$ cells) was observed at 0.25μM, 0.5μM and 1μM concentrations of poloxipan. The 0.25μM and 1μM treatments were also significant (n=4).

Poloxipan did have a dose dependent effect that at the highest concentration (4.0μM) was sufficient to lower the MCF10A viability to a normalised value of 0.63 in the MCF10A cells. A further increase in the concentration of Poloxipan would have reduced the viability to a normalised value of <0.50.

The *CDH1*$^{-/-}$ cells treated with 2μM and 4μM concentrations of poloxipan showed that the *CDH1*$^{-/-}$ cells were less viable than the MCF10A cells. The synthetic lethal viability ratio was not met and therefore the inhibition of

PLK3 with poloxipan in *CDH1*$^{-/-}$ cells is not synthetic lethal. The p-values also indicate that this was not a significant effect (n=4) (Table 9).

Table 9 – Average Viability of MCF10A and *CDH1*$^{-/-}$ cells to poloxipan treatment normalised to the DMSO control. The standard error (STD Error) of the viability; the viability ratio; and the p-values of the poloxipan treatment are also indicated.

Poloxipan Treatment						
	MCF10A		*CDH1*$^{-/-}$		Viability Ratio	P-Value
	Viability	STD Error	Viability	STD Error		
0.25µM	0.95	0.04	1.10	0.07	1.16	0.02
0.5µM	1.01	0.03	1.10	0.09	1.10	0.16
1.0µM	0.92	0.02	1.09	0.04	1.08	0.00
2.0µM	0.97	0.12	0.91	0.08	0.94	0.08
4.0µM	0.63	0.22	0.61	0.14	0.97	0.43

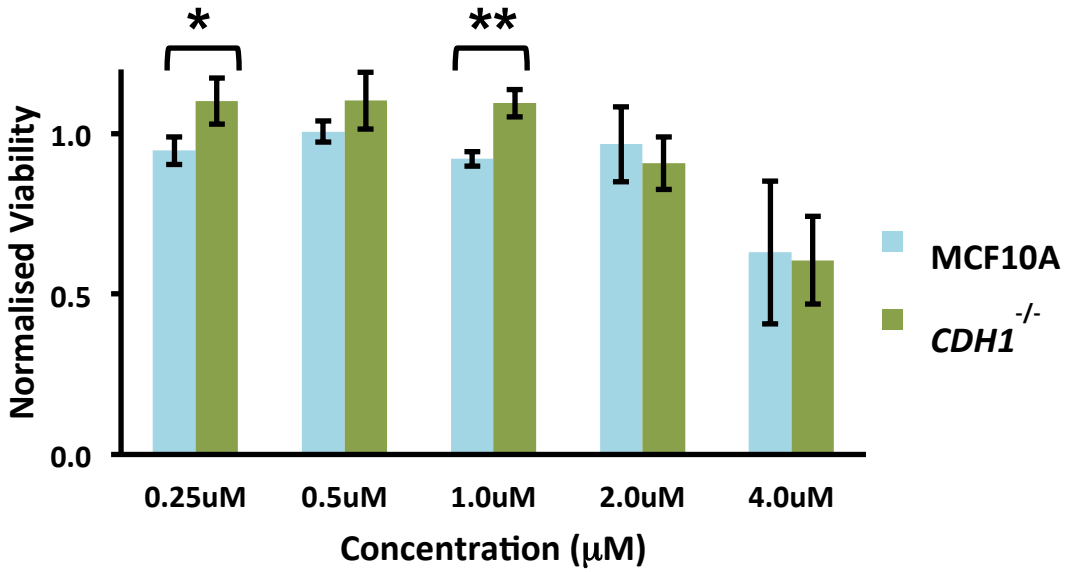

Figure 19 - Average of the normalised viability of MCF10A and *CDH1*$^{-/-}$ cells after treatment with poloxipan. Poloxipan treatment was in 0.25µM, 0.5µM, 1.0µM, 2.0µM and 4.0µM concentrations. Four biological repeats each with six technical repeats. Cells were treated 24 hrs after seeding and viability measured from total cell count at 48 hrs after treatment. Total cell count was normalised to the DMSO control. * = p-value <0.05; ** = p-value <0.01.

3.3 WORTMANNIN

In the same pattern as poloxipan (Chapter 2.5), wortmannin was administered to the MCF10A and *CDH1*$^{-/-}$ cells and imaged in the IncuCyte to measure confluence changes over time. The images show the behaviour of the cells before and after treatment of poloxipan. Cells were treated 24 hrs after seeding, and stained and imaged to count the nuclei at 48 hrs. The total cell count was normalised to the DMSO control for determination of cell viability in response to treatment.

Wortmannin is a PI3K inhibitor with and IC_{50} value of 3.0nM that also inhibits PLK3. It has been well characterised and used in many in vitro and in vivo studies. Different isoforms are in clinical trials for those who have PI3K driven tumours. Wortmannin is treated at concentrations at which it is known to inhibit PLK3 and PLK1. The IC_{50} values of wortmannin for PLK3 are 48nM and 5.8nM for PLK1. Our experiment optimised wortmannin to be treated at 0.63μM, 1.25μM, 2.5μM, 5.0μM, and 10.0μM.

3.3.1 GROWTH OF WORTMANNIN TREATED CELLS

Wortmannin caused a significant growth inhibition and a decrease in cell confluence within the first 2 hrs of treatment. The effect of wortmannin had a dose-dependent relationship (**Figure 20**). The cells treated with a lower concentration of wortmannin recovered to the normal growth rate observed in the DMSO control, quicker than cells treated at a higher dose. Wortmannin affected both MCF10A and *CDH1*$^{-/-}$, but *CDH1*$^{-/-}$ had a greater

lethality indicative of a synthetic lethal relationship between *CDH1* and wortmannin's targets.

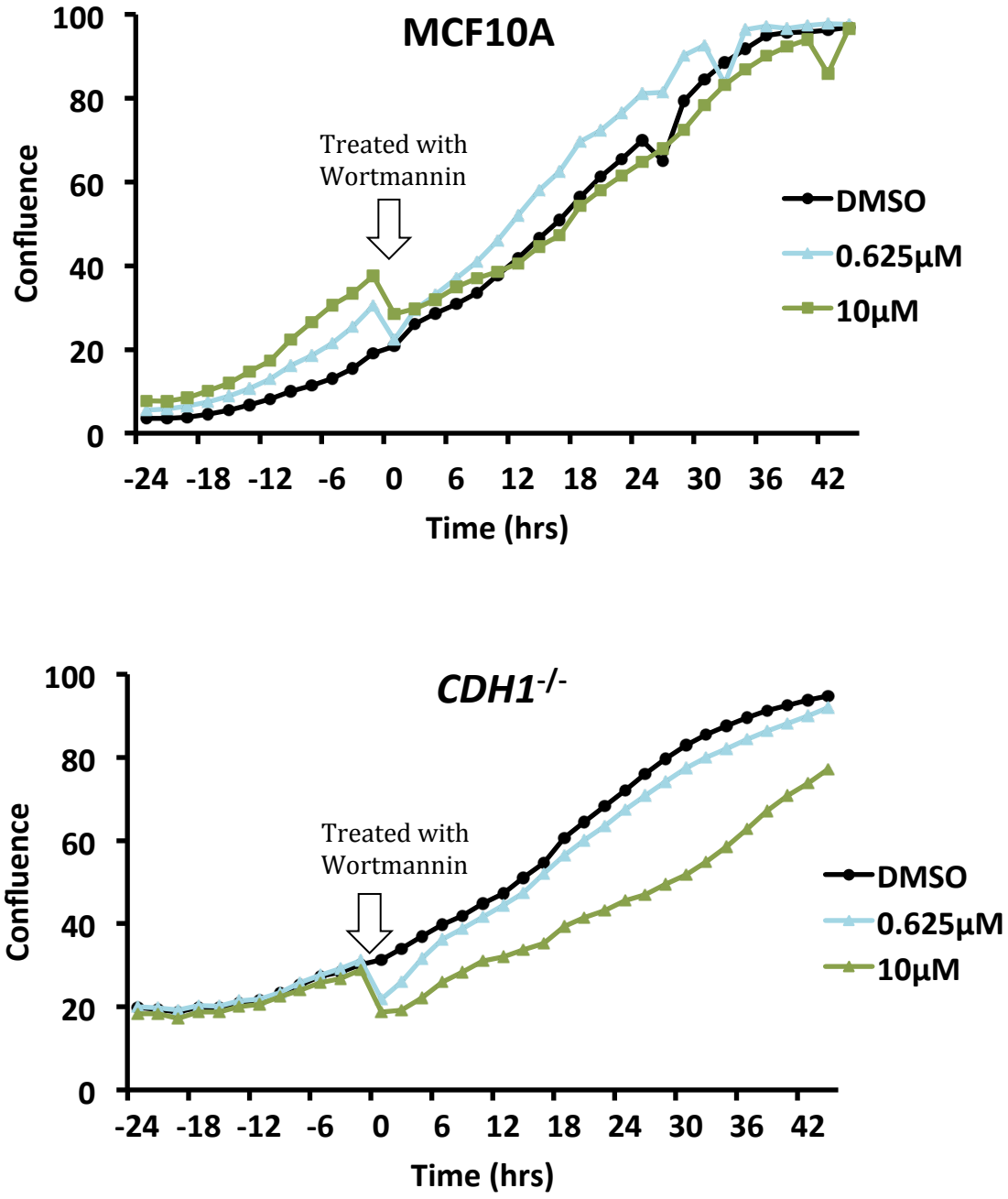

Figure 20 – Pre and post treatment confluence over time of MCF10A and *CDH1*$^{-/-}$ cells treated with 10µM of wortmannin After time 0, cells were treated with a range of concentrations of Wortmannin of which 0.625µM and 10µM are shown in comparison to the DMSO control.

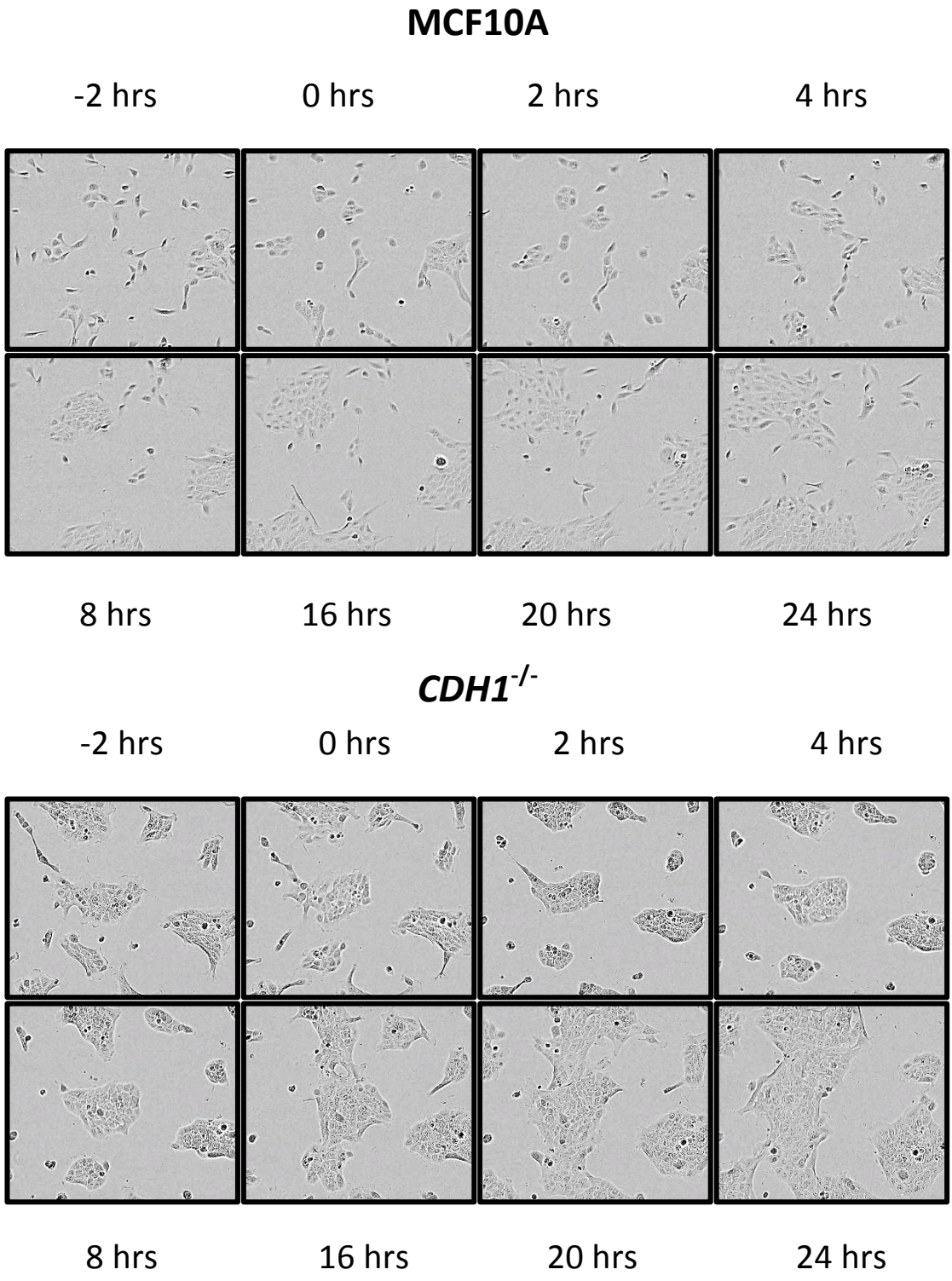

Figure 21 - Images of the MCF10A and *CDH1*$^{-/-}$ cells before and after treatment of 10µM of wortmannin. The MCF10A images were from well B11 and the 1st field of view. The *CDH1*$^{-/-}$ images were from well E11, and the 3rd field of view. Images were taken in the IncuCyte every 2 hrs of which the -2, 0, 4, 8,16, 20, and 24 hour time points are shown. Treatment of Wortmannin occurred after the 0 hrs, the first response is seen at 2 hrs.

The images obtained from the IncuCyte (**Figure 21**) showed that wortmannin treatment rendered the migrating and isolated MCF10A and *CDH1*$^{-/-}$ cells unable to grow. *CDH1*$^{-/-}$ cells clumped together and existing clumps were reduced in size. After 16 hrs *CDH1*$^{-/-}$ cells were again growing. There clumped MCF10A cells that had no immediate effect in the first 4 hrs. The lack of growth is more evident in the *CDH1*$^{-/-}$ cells and indicates that wortmannin treatment is lethal to

3.3.2 VIABILITY OF WORTMANNIN TREATED CELLS

48 hrs after the wortmannin treatment, cells were imaged in the Cytation to calculate the total cell count. The cell count of each treatment was normalised to the equivalent DMSO of that cell line, which provided the viability as conducted I', meaning we must accept the null hypothesis. We can conclude that there is no collaborating significant synthetic lethal relationship or reverse synthetic lethal relationship between wortmannin and *CDH1*$^{-/-}$ cells.

Table 10 – Average Viability of MCF10A and *CDH1*$^{-/-}$ cells after wortmannin treatment, normalised to the DMSO control. The standard error (STD Error) of the viability; the viability ratio; and p-values of the wortmannin treatment.

Wortmannin Treatment						
	MCF10A		*CDH1*$^{-/-}$		Viability Ratio	P-Value
	Viability	STD Error	Viability	STD Error		
0.63μM	0.97	0.08	1.00	0.04	1.03	0.41
1.25μM	0.88	0.13	0.86	0.07	0.98	0.45
2.5μM	0.87	0.03	0.81	0.03	0.93	0.14
5.0μM	0.82	0.06	0.83	0.02	1.01	0.47
10.0μM	0.62	0.10	0.64	0.06	1.03	0.47

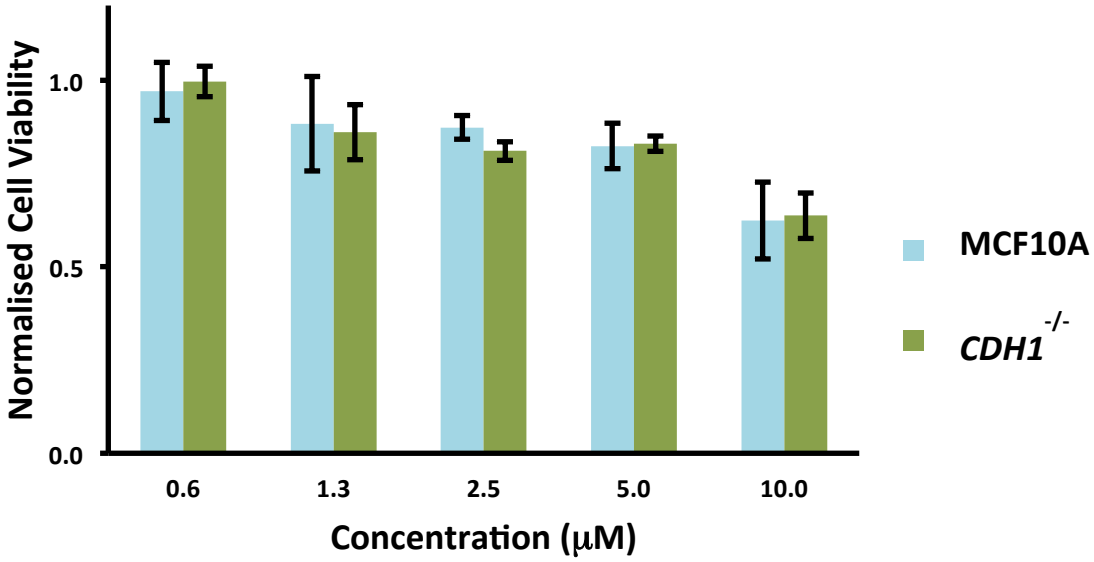

Figure 22 - Average of the normalised viability of MCF10A and *CDH1*$^{-/-}$ cells after treatment with wortmannin (µM). Concentrations of wortmannin were 0.6µM, 1.3µM, 2.5µM, 5.0µM and 10µM. Cells were treated 24 hrs after seeding. Staining and counting occurred at 48 hrs after treatment. The total cell count of 6 technical repeats was normalised to the average of the DMSO control.

4 DISCUSSION

"For me, I am driven by two main philosophies: Know more today about the world than I knew yesterday and lessen the suffering of others. You'd be surprised how far that gets you." – Neil deGrasse Tyson

The synthetic lethal response between *CDH1*$^{-/-}$ cells and *PLK3* knockdown found in the high throughput siRNA screen conducted in our lab needed validation [27]. This screen found that a knockdown of *PLK3* caused a viability ratio of 0.84, with *CDH1*$^{-/-}$ cells being less viable than their isogenic MCF10A partner. The threshold to be considered a synthetic lethal candidate was to have a viability ratio less than 0.85. *PLK3* also had biological relevance to microtubule-associated proteins that were identified frequently as having a synthetic lethal affect on *CDH1*$^{-/-}$ cells.

Finding a synthetic lethal candidate would be of great benefit to the hundreds of families (including the families here in New Zealand) that carry a *CDH1* mutation. Currently HDGC is treated by a total prophylactic gastrectomy to remove their stomach and remove their 70% likelihood of developing diffuse gastric cancer. Gastrectomy has a 100% chance of surgical morbidity, and can have serious metabolic consequences leading to multiple malnutrition problems [74]. Hormones that regulate hunger (ghrelin and leptin) that are produced by the stomachs epithelial lining become deficient. Eating too much without a stomach can lead to gastric reflux, as they do not have the capacity to store as much food. Vitamin B_{12} deficiency leading to megaloblastic anaemia is a malnutrition risk which

requires regular supplement injections [75]. If a woman has HDGC she is also prone to developing lobular breast cancer. In addition, their quality of life can be affected by increased antisocial behaviour, pain, fatigue, anxiety, and reduced self esteem from body image [76].To reduce the burden of all these conditions an alternative preventative is needed.

A perfect synthetic lethal vulnerability will have minimised effect on normal cells that means limited toxicity to the patient. Ideally, only the cells with the sporadic second hit and inactive *CDH1* will be killed by the treatment. This potential treatment course could be repeated at regular intervals to keep the patient free of advanced disease. With much progress in identifying biologically plausible targets from the original siRNA screen, it is only a matter of time before we find the right target and the right compound. In the mean time, understanding genes with the *CDH1* association that cause synthetic lethality (such as the microtubule association *PLK3* regulated) will aid this research effort.

4.1 *PLK3* KNOCKDOWN BY SHRNA

The successful knockdown of *PLK3* from the transduction of shRNA E4 caused a viability ratio of 1.65, meaning it had a strong reverse synthetic lethal relationship. The standard error of this relationship was broad and the p-value was not significant. The E7 shRNA likewise was not significant and did not show a synthetic lethal relationship from the viability ratio of 0.92.

This was not a significant relationship and requires further biological repeats confirming a *PLK3* knockdown to answer if there indeed were a reverse synthetic lethal relationship. This is because the E7 shRNA, which had more biological repeats, did not cause the same effect as the E4 shRNA, which does not validating the specific effect. Both experiments confirmed a knockdown of *PLK3* but the variation in viability was substantial. Additional knockdown repeats are needed but it is most likely the relationship is not substantial.

Error in the expression of the housekeeping gene *PPIA* in the RT-qPCR reaction may have been influenced by that fact that multiple products appeared on the gel. This indicates the *PPIA* primers may not have been efficient. The efficiency of three RT-qPCR reactions was higher than an two, meaning a doubling. A reaction that produces more than double each cycle is not possible and is skewed by errors in the standard. These results were discarded as unable to validate. Repeating RT-qPCR a second time for each transduction was not achievable as all the cDNA was used up to provide triplicate replicates. This meant a whole new transduction had to be carried out, which considering the growing time of the cells was a time consuming task that had no room for error from any inadequacies or incapability.

The variability in the shRNA synthetic lethal effect can be caused by a multitude of factors. The original siRNA screen showed the *PLK3* knockdown was only synthetic lethal in 2/4 of the siRNA sequences (Table 2 and **Figure 3**). The siRNA sequences all were targeting the same gene, but

there is potential that some sequences are a better match and are more effective in the knockdown than others. Confirming the knockdown was meant to eliminate this error, but the variability remained.

Unfortunately targeting a knockdown of *PLK3* for synthetic lethality was not able to advance any therapeutic leads. These results do aid in future efforts to validate synthetic lethality in other potential targets; the viability ratio can be raised to a stricter threshold based on this validation of *PLK3*. The original screen identified *PLK3* as a target by meeting the viability ratio threshold of 0.85 but it eventuated to be non-significant. A threshold of 0.75 would have greater power to exclude the noise. Results of the *PLK3* knockdown caused fluctuations in the cell viability without having any consistency. This is also reflected in the originally individual siRNA results. The screen was conducted at a high throughput and may have the potential to miss important key players, which only was an outlier primarily. Including the smaller synthetic lethal effects at a 0.85 threshold may have included one of these outliers with potential to show a greater synthetic lethal effect. This was not the case with *PLK3*.

4.2 PLK3 INHIBITORS

4.2.1 POLOXIPAN

Poloxipan is a pan inhibitor of the polo-like kinase family meaning it is not specific to *PLK3*. PLK1 is a tumour promoter because of its suppression on p53 that is being researched in various cancers. More specific inhibitors of PLK1 are currently in phase I and II trials. PLK1 is an agonist of PLK3. PLK3

is the tumour suppressor that activates p53 causing cell cycle arrest and apoptosis. Considering that poloxipan inhibited both of these Polo-like kinases, the inconsistency and non-significant effects are not too surprising. The only significant relationship that was determined was the reverse synthetic lethal relationship at low concentrations of poloxipan. Increasing the concentration of poloxipan only decreased the viability of both MCF10A and *CDH1*$^{-/-}$ cells and was no longer reverse synthetic lethal.

4.3 REVERSE SYNTHETIC LETHALITY

A reverse synthetic lethal treatment can be induced in several ways. When the MCF10A cell line was intended to be unaffected, treatment can be reverse synthetic lethal by either killing the MCF10A cells to a greater extent than the *CDH1*$^{-/-}$ cells. The other way a treatment can be reverse synthetic lethal is if it causes *CDH1*$^{-/-}$ cells to proliferate and grow more than the MCF10A and control. As *CDH1*$^{-/-}$ cells represent the HDGC tumour cells a reverse synthetic lethal relationship is therefore one that would promote tumour growth and is to be fully avoided in any treatment.

The fact that this trend was seen for the E4 shRNA is potentially very problematic for any case promoting *PLK3* knockdown as a treatment. One implication returns to the danger of using PLK1 drug inhibitors. Current PLK1 inhibitors are not exclusive to PLK1 and often inhibit PLK3 at the same concentrations at which they target PLK1. Such a relationship was one of the reasons why wortmannin was tested in this experiment as this PI3K inhibitor also has off target effects on PLK1 and PLK3 at similar

concentrations at which it would be inhibiting PI3K. The success of wortmannin treatment for cancer, inflammation, immunology and cardiovascular disease may have been influenced by the polo-like kinase inhibition [69].

4.4 FUTURE DIRECTIONS

PLK3 should no longer be considered a strong synthetic lethal candidate for E-cadherin negative cancers. However the results were not consistent and further validation of this relationship can be done. Further transductions with shRNA knockdowns are needed, with confirmation of *PLK3* knockdown. Knocking down the *PLK3* mRNA doesn't exclude residual PLK3 proteins from affecting the cells. Validating whether the knockdown led to a PLK3 deficient cell could be investigated by a western blot. *PLK3* as a cell cycle regulator and is signalled to be expressed every cycle. It can be anticipated that presence of existing PLK3 will decrease after a few completed replications.

The IncuCyte images showed poloxipan and wortmannin treatments caused a lethal effect on *CDH1*$^{-/-}$ cells immediately after treatment. The same response was not seen to the same degree in MCF10A cells. There remains potential for a synthetic lethal effect from poloxipan and wortmannin, although it could arguably be from inhibition of PLK1 or PI3K and not PLK3. Determining the viability at 48 hrs after treatment could have allowed cell colonies to continue to proliferate and masked any true effect the inhibitors do produce. Conducting a cell luminescence assay

determining the amount of viable cells at multiple time points would reveal the effect these inhibitors have on viability. Multiple dosages every two – three hrs could also enhance any potential existing synthetic lethal relationship.

The clumping of the cells in response to PLK3 inhibition was also of interest as this occurred to a greater extent in the *CDH1*$^{-/-}$ cell line. Performing a scratch assay and finding the migration times for each cell line in response to the treatment would have been of interest. The clumping could also have limited the amount of drug that was able to influence the cell and could have provided some of the inconsistencies across the data. The clumping could be indicative that PLK3 loss alters cell migration.

Attempts to determine if the effect of *PLK3* knockdown/inhibition was lethal compared to only inhibitive of growth were not consistently recorded. Propidium iodide staining served as an indicator of the amount of dead cells and was available for two of the successful experiments. Repeating the transduction and inhibition can be repeated to derive what the true lethal response is. Cells may still be viable but could have been in cell cycle arrest. The plates were confluent so cell growth continued to occur, as they were not seeded or treated at confluence. Determining the stage of the cell cycle through 10x images on the Cytell would have been beneficial to observe from the PLK3 inhibitor treatments. Including further time points providing the immediate response to treatment would also greatly assist this validation.

4.5 SUMMARY

There is no significant synthetic lethal relationship between *CDH1* and *PLK3*.

The successful knockdown of *PLK3* using lentiviral delivery of shRNA resulted in a reverse synthetic lethal relationship from the E4 shRNA sequence, and a lethal effect to both cell lines from the E7 shRNA sequence. The p-values indicate that the results were non-significant.

Inhibiting PLK3 with the inhibitors poloxipan and wortmannin and testing viability from total cell count 48 hrs later did not provide a synthetic lethal relationship. Images and the confluence measure indicated that *CDH1*$^{-/-}$ cells were subject to a greater growth inhibition. This information remains to be quantified and validated and is not necessarily due to the inhibition of *PLK3*.

These experiments indicate that PLK3 is not a strong synthetic lethal candidate for E-cadherin deficient cancers. As PLK3 was representative of microtubule associated regulators, this provides an insight that this association may not be the vulnerability that needs to be targeted. This validation enables further more accurate assessments of the remaining synthetic lethal candidates.

5 APPENDIX

5.1 LYSOGENY BROTH AGAR PLATES

Autoclave the 100mL of LB with 1.5% agar (Appendix 5.2) for one hour. 100mL of LB with 1.5% agar is sufficient for 3 agar plates. Once cool, add 200μL of 50mg/mL ampicillin to obtain 100μg/mL and swirl gently. Pour about 30mL of the agar and ampicillin mix into a 94mm × 16mm, vented disposable petri dish (BRAND). This can be used for up to 3 days if kept in 4°C. Allow to. Warm at room temperature before streaking with *E.coli*.

5.2 LYSOGENY BROTH COMPONENTS

Combine substrates in a 1L beaker and mix the substrates together using a magnetic stirrer. Pour 100mL into a 200mL Schott bottle, 200mL into a 400mL Schott bottle and 200mL into a second 400mL Schott bottle.

Table 11 - Components of Lysogeny Broth

Lysogeny Broth	
Component:	**Quantity:**
Tryptone	5g
Yeast Extract	2.5g
NaCl	10g
MQ H_2O	500mL
Total	500mL ~ 16 plates

5.3 RT-qPCR PRIMERS

Table 12 – The sequences of the RT-qPCR reactions primers. * = Primers were pre-designed by Integrated DNA Technologies (IDT).

Target	Forward	Reverse
GAPDH*	GCGCCAATACGACCAA	GCTCTCTGCTCCTCCTGTT
***PPIA** **	TCTTTCACTTTGCCAAACACC	CATCCTAAAGCATACGGGTCC
PLK3	GCGCGAGAAGATCCTAAATG	TTGTCAGCGTCCTCAAAGTG

5.4 E7 SHRNA KNOCKDOWN

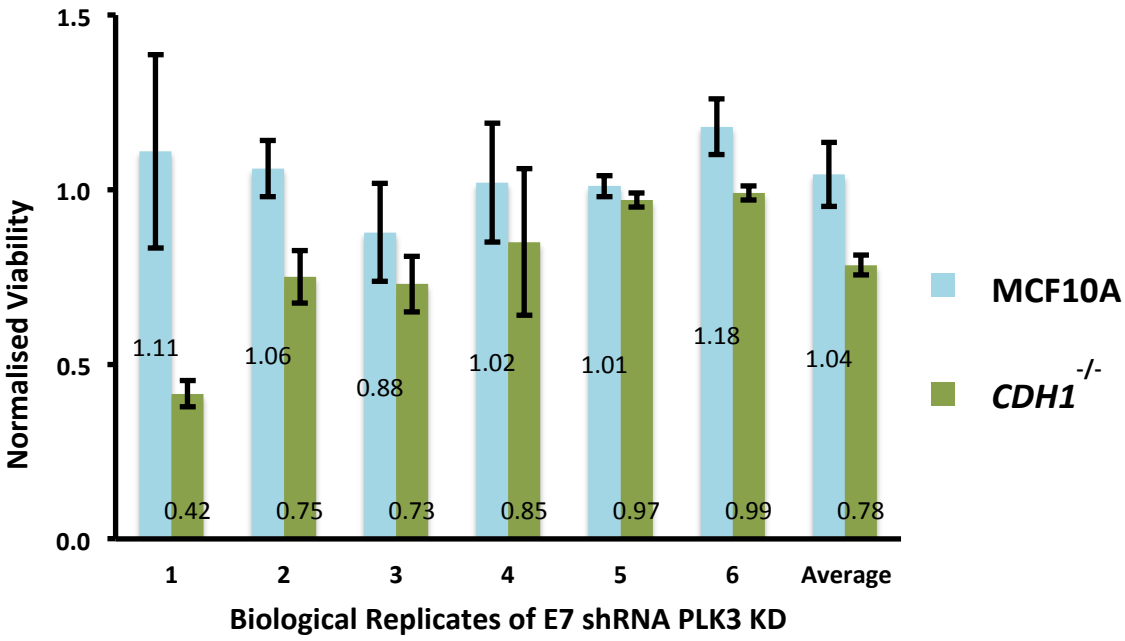

Figure 23 – Average of the viability after E7 shRNA attempted *PLK3* knockdown

6 REFERENCES

1 Guilford, P., Humar, B. and Blair, V. (2010) Hereditary diffuse gastric cancer: translation of CDH1 germline mutations into clinical practice. Gastric Cancer **13**, 1–10.

2 Chen, A., Beetham, H., Black, M. A., Priya, R., Telford, B. J., Guest, J., Wiggins, G. A. R., Godwin, T. D., Yap, A. S. and Guilford, P. J. (2014) E-cadherin loss alters cytoskeletal organization and adhesion in non-malignant breast cells but is insufficient to induce an epithelial-mesenchymal transition. BMC Cancer **14**, 552–14.

3 Reindl, W., Yuan, J., Kramer, A., Strebhardt, K. and Berg, T. (2009) A pan-specific inhibitor of the polo-box domains of polo-like kinases arrests cancer cells in mitosis. Chembiochem **10**, 1145–1148.

4 Guilford, P. J., Hopkins, J. B., Grady, W. M., Markowitz, S. D., Willis, J., Lynch, H., Rajput, A., Wiesner, G. L., Lindor, N. M., Burgart, L. J., et al. (1999) E-cadherin germline mutations define an inherited cancer syndrome dominated by diffuse gastric cancer. Hum Mutat, John Wiley & Sons, Inc. **14**, 249–255.

5 Kaurah, P., MacMillan, A., Boyd, N., Senz, J., De Luca, A., Chun, N., Suriano, G., Zaor, S., Van Manen, L., Gilpin, C., et al. (2007) Founder and recurrent CDH1 mutations in families with hereditary diffuse gastric cancer. JAMA, American Medical Association **297**, 2360–2372.

6 Lehnert, T. and Buhl, K. (2004) Techniques of reconstruction after total gastrectomy for cancer. Br J Surg **91**, 528–539.

7 Jones, E. G. (1964) FAMILIAL GASTRIC CANCER. N Z Med J **63**, 287–296.

8 Oliveira, C., Pinheiro, H., Figueiredo, J., Seruca, R. and Carneiro, F. (2015) Familial gastric cancer: genetic susceptibility, pathology, and implications for management. Lancet Oncol **16**, e60–70.

9 Machado, J. C., Oliveira, C., Carvalho, R., Soares, P., Berx, G., Caldas, C., Seruca, R., Carneiro, F. and Sobrinho-Simoes, M. (2001) E-cadherin gene (CDH1) promoter methylation as the second hit in sporadic diffuse gastric carcinoma. Oncogene **20**, 1525–1528.

10 Barber, M. E., Save, V., Carneiro, F., Dwerryhouse, S., Lao-Sirieix, P., Hardwick, R. H., Caldas, C. and Fitzgerald, R. C. (2008) Histopathological and molecular analysis of gastrectomy specimens from hereditary diffuse gastric cancer patients has implications for endoscopic surveillance of individuals at risk. J Pathol **216**, 286–294.

11 Nordling, C. O. (1953) A new theory on cancer-inducing mechanism. Br J Cancer **7**, 68–72.

12 Tamura, G., Yin, J., Wang, S., Fleisher, A. S., Zou, T., Abraham, J. M., Kong, D., Smolinski, K. N., Wilson, K. T., James, S. P., et al. (2000) E-Cadherin gene promoter hypermethylation in primary human gastric carcinomas. J Natl Cancer Inst **92**, 569–573.

13 Pinheiro, H., Oliveira, C., Seruca, R. and Carneiro, F. (2014) Hereditary

diffuse gastric cancer - pathophysiology and clinical management. Best Pract Res Clin Gastroenterol **28**, 1055–1068.
14 Pedrazzani, C., Corso, G., Marrelli, D. and Roviello, F. (2007) E-cadherin and hereditary diffuse gastric cancer. Surgery **142**, 645–657.
15 Oliveira, C., Senz, J., Kaurah, P., Pinheiro, H., Sanges, R., Haegert, A., Corso, G., Schouten, J., Fitzgerald, R., Vogelsang, H., et al. (2009) Germline CDH1 deletions in hereditary diffuse gastric cancer families. Hum Mol Genet **18**, 1545–1555.
16 Lynch, H. T., Grady, W., Suriano, G. and Huntsman, D. (2005) Gastric cancer: new genetic developments. J Surg Oncol **90**, 114–33– discussion 133.
17 Jakubowska, A., Lawniczak, M., Wojnarska, B., Cybulski, C., Huzarski, T., Byrski, T., Toloczko-Grabarek, A., Jaworska, K., Durda, K., Starzynska, T., et al. (2010) CDH1 gene mutations do not contribute in hereditary diffuse gastric cancer in Poland. Fam Cancer **9**, 605–608.
18 Majewski, I. J., Kluijt, I., Cats, A., Scerri, T. S., de Jong, D., Kluin, R. J. C., Hansford, S., Hogervorst, F. B. L., Bosma, A. J., Hofland, I., et al. (2013) An alpha-E-catenin (CTNNA1) mutation in hereditary diffuse gastric cancer. J Pathol **229**, 621–629.
19 Caldas, C., Carneiro, F., Lynch, H. T., Yokota, J., Wiesner, G. L., Powell, S. M., Lewis, F. R., Huntsman, D. G., Pharoah, P. D., Jankowski, J. A., et al. (1999) Familial gastric cancer: overview and guidelines for management. Journal of Medical Genetics **36**, 873–880.
20 Fitzgerald, R. C., Hardwick, R., Huntsman, D., Carneiro, F., Guilford, P., Blair, V., Chung, D. C., Norton, J., Ragunath, K., Van Krieken, J. H., et al. (2010) Hereditary diffuse gastric cancer: updated consensus guidelines for clinical management and directions for future research. Journal of Medical Genetics **47**, 436–444.
21 el-Zimaity, H. M., Itani, K. and Graham, D. Y. (1997) Early diagnosis of signet ring cell carcinoma of the stomach: role of the Genta stain. J Clin Pathol **50**, 867–868.
22 Charlton, A., Blair, V., Shaw, D., Parry, S., Guilford, P. and Martin, I. G. (2004) Hereditary diffuse gastric cancer: predominance of multiple foci of signet ring cell carcinoma in distal stomach and transitional zone. Gut **53**, 814–820.
23 Blair, V., Martin, I., Shaw, D., Winship, I., Kerr, D., Arnold, J., Harawira, P., McLeod, M., Parry, S., Charlton, A., et al. (2006) Hereditary diffuse gastric cancer: diagnosis and management. Clin Gastroenterol Hepatol **4**, 262–275.
24 Corso, G., Figueiredo, J., Biffi, R., Trentin, C., Bonanni, B., Feroce, I., Serrano, D., Cassano, E., Annibale, B., Melo, S., et al. (2014) E-cadherin germline mutation carriers: clinical management and genetic implications. Cancer Metastasis Rev, Springer US **33**, 1081–1094.
25 van Roy, F. and Berx, G. (2008) The cell-cell adhesion molecule E-cadherin. Cell. Mol. Life Sci. **65**, 3756–3788.
26 Lu, M., Marsters, S., Ye, X., Luis, E., Gonzalez, L. and Ashkenazi, A. (2014) E-Cadherin Couples Death Receptors to the Cytoskeleton to Regulate Apoptosis. Molecular Cell, Elsevier Inc. **54**, 987–998.
27 Telford, B. J., Chen, A., Beetham, H., Frick, J., Brew, T. P., Gould, C. M.,

Single, A., Godwin, T., Simpson, K. J. and Guilford, P. (2015) Synthetic Lethal Screens Identify Vulnerabilities in GPCR Signaling and Cytoskeletal Organization in E-Cadherin-Deficient Cells. Molecular Cancer Therapeutics **14**, 1213–1223.
28 Xu, D., Wang, Q., Jiang, Y., Zhang, Y., Vega-Saenzdemiera, E., Osman, I. and Dai, W. (2012) Roles of Polo-like kinase 3 in suppressing tumor angiogenesis. Exp Hematol Oncol, BioMed Central Ltd **1**, 5.
29 Takeichi, M. (1977) Functional correlation between cell adhesive properties and some cell surface proteins. The Journal of Cell Biology **75**, 464–474.
30 Hyafil, F., Babinet, C. and Jacob, F. (1981) Cell-cell interactions in early embryogenesis: a molecular approach to the role of calcium. Cell **26**, 447–454.
31 Ogou, S. I., Yoshida-Noro, C. and Takeichi, M. (1983) Calcium-dependent cell-cell adhesion molecules common to hepatocytes and teratocarcinoma stem cells. The Journal of Cell Biology **97**, 944–948.
32 Yoshida-Noro, C., Suzuki, N. and Takeichi, M. (1984) Molecular nature of the calcium-dependent cell-cell adhesion system in mouse teratocarcinoma and embryonic cells studied with a monoclonal antibody. Dev Biol **101**, 19–27.
33 Du, W., Liu, X., Fan, G., Zhao, X., Sun, Y., Wang, T., Zhao, R., Wang, G., Zhao, C., Zhu, Y., et al. (2014) From cell membrane to the nucleus: an emerging role of E-cadherin in gene transcriptional regulation. J Cell Mol Med **18**, 1712–1719.
34 Priya, R. and Yap, A. S. (2015) Active tension: the role of cadherin adhesion and signaling in generating junctional contractility. Curr Top Dev Biol **112**, 65–102.
35 Lecuit, T. and Yap, A. S. (2015) E-cadherin junctions as active mechanical integrators in tissue dynamics. Nat Cell Biol **17**, 533–539.
36 Miyoshi, J. and Takai, Y. (2009) Adherens Junctions. In Encyclopedia of Cancer, pp 53–57, Springer Berlin Heidelberg, Berlin, Heidelberg.
37 Becker, K. F., Atkinson, M. J., Reich, U., Huang, H. H., Nekarda, H., Siewert, J. R. and Hofler, H. (1993) Exon skipping in the E-cadherin gene transcript in metastatic human gastric carcinomas. Hum Mol Genet **2**, 803–804.
38 Wijnhoven, B. P., de Both, N. J., van Dekken, H., Tilanus, H. W. and Dinjens, W. N. (1999) E-cadherin gene mutations are rare in adenocarcinomas of the oesophagus. Br J Cancer **80**, 1652–1657.
39 Levenson, A. S. and Jordan, V. C. (1997) MCF-7: the first hormone-responsive breast cancer cell line. Cancer Research **57**, 3071–3078.
40 Nijman, S. M. B. (2011) Synthetic lethality: general principles, utility and detection using genetic screens in human cells. FEBS Lett **585**, 1–6.
41 (2010) Synthetic lethal approaches to breast cancer therapy, Nature Publishing Group **7**, 718–724.
42 Yoshida, K. and Miki, Y. (2004) Role of BRCA1 and BRCA2 as regulators of DNA repair, transcription, and cell cycle in response to DNA damage. Cancer Sci **95**, 866–871.
43 Farmer, H., McCabe, N., Lord, C. J., Tutt, A. N. J., Johnson, D. A.,

Richardson, T. B., Santarosa, M., Dillon, K. J., Hickson, I., Knights, C., et al. (2005) Targeting the DNA repair defect in BRCA mutant cells as a therapeutic strategy. Nature, Macmillian Magazines Ltd. **434**, 917–921.
44 Zitouni, S., Nabais, C., Jana, S. C., Guerrero, A. and Bettencourt-Dias, M. (2014) Polo-like kinases: structural variations lead to multiple functions, Nature Publishing Group **15**, 433–452.
45 Liu, X. and Erikson, R. L. (2003) Polo-like kinase (Plk)1 depletion induces apoptosis in cancer cells. Proc Natl Acad Sci U S A **100**, 5789–5794.
46 Johnson, E. F., Stewart, K. D., Woods, K. W., Giranda, V. L. and Luo, Y. (2007) Pharmacological and Functional Comparison of the Polo-like Kinase Family: Insight into Inhibitor and Substrate Specificity. Biochemistry **46**, 9551–9563.
47 Strebhardt, K. (2010) Multifaceted polo-like kinases: drug targets and antitargets for cancer therapy, Nature Publishing Group 1–18.
48 Bahassi, E. M., Conn, C. W., Myer, D. L., Hennigan, R. F., McGowan, C. H., Sanchez, Y. and Stambrook, P. J. (2002) Mammalian Polo-like kinase 3 (Plk3) is a multifunctional protein involved in stress response pathways. Oncogene **21**, 6633–6640.
49 Xie, S., Xie, B., Lee, M. Y. and Dai, W. (2005) Regulation of cell cycle checkpoints by polo-like kinases. Oncogene **24**, 277–286.
50 Xie, S. (2001) Plk3 Functionally Links DNA Damage to Cell Cycle Arrest and Apoptosis at Least in Part via the p53 Pathway. Journal of Biological Chemistry **276**, 43305–43312.
51 Loffler, H., Lukas, J., Bartek, J. and Kramer, A. (2006) Structure meets function--centrosomes, genome maintenance and the DNA damage response. Exp Cell Res **312**, 2633–2640.
52 Xu, D., Yao, Y., Lu, L., Costa, M. and Dai, W. (2010) Plk3 Functions as an Essential Component of the Hypoxia Regulatory Pathway by Direct Phosphorylation of HIF-1. Journal of Biological Chemistry **285**, 38944–38950.
53 Xu, D., Yao, Y., Jiang, X., Lu, L. and Dai, W. (2010) Regulation of PTEN Stability and Activity by Plk3. Journal of Biological Chemistry **285**, 39935–39942.
54 Wang, Q., Xie, S., Chen, J., Fukasawa, K., Naik, U., Traganos, F., Darzynkiewicz, Z., Jhanwar-Uniyal, M. and Dai, W. (2002) Cell cycle arrest and apoptosis induced by human Polo-like kinase 3 is mediated through perturbation of microtubule integrity. Molecular and Cellular Biology **22**, 3450–3459.
55 Jiang, N., Wang, X., Jhanwar-Uniyal, M., Darzynkiewicz, Z. and Dai, W. (2006) Polo box domain of Plk3 functions as a centrosome localization signal, overexpression of which causes mitotic arrest, cytokinesis defects, and apoptosis. Journal of Biological Chemistry **281**, 10577–10582.
56 Iida, M., Sasaki, T. and Komatani, H. (2009) Overexpression of Plk3 causes morphological change and cell growth suppression in Ras pathway-activated cells. J Biochem **146**, 501–507.
57 Naik, M. U. and Naik, U. P. (2011) Calcium- and integrin-binding protein 1 regulates microtubule organization and centrosome

segregation through polo like kinase 3 during cell cycle progression. Int J Biochem Cell Biol **43**, 120–129.
58 Fire, A., Xu, S., Montgomery, M. K., Kostas, S. A., Driver, S. E. and Mello, C. C. (1998) Potent and specific genetic interference by double-stranded RNA in Caenorhabditis elegans. Nature **391**, 806–811.
59 Moore, C. B., Guthrie, E. H., Huang, M. T.-H. and Taxman, D. J. (2010) Short hairpin RNA (shRNA): design, delivery, and assessment of gene knockdown. Methods Mol Biol **629**, 141–158.
60 Xiang, S., Fruehauf, J. and Li, C. J. (2006) Short hairpin RNA|[ndash]|expressing bacteria elicit RNA interference in mammals. Nat Biotech, Nature Publishing Group **24**, 697–702.
61 Rao, D. D., Vorhies, J. S., Senzer, N. and Nemunaitis, J. (2009) siRNA vs. shRNA: similarities and differences. Adv Drug Deliv Rev **61**, 746–759.
62 Okimoto, T., Friedmann, T. and Miyanohara, A. (2001) VSV-G envelope glycoprotein forms complexes with plasmid DNA and MLV retrovirus-like particles in cell-free conditions and enhances DNA transfection. Mol Ther **4**, 232–238.
63 Dalby, B., Cates, S., Harris, A., Ohki, E. C., Tilkins, M. L., Price, P. J. and Ciccarone, V. C. (2004) Advanced transfection with Lipofectamine 2000 reagent: primary neurons, siRNA, and high-throughput applications. Methods **33**, 95–103.
64 Cockrell, A. S. and Kafri, T. (2007) Gene delivery by lentivirus vectors. Mol Biotechnol **36**, 184–204.
65 Lambeth, L. S. and Smith, C. A. (2013) Short hairpin RNA-mediated gene silencing. Methods Mol Biol **942**, 205–232.
66 Soule, H. D., Maloney, T. M., Wolman, S. R., Peterson, W. D. J., Brenz, R., McGrath, C. M., Russo, J., Pauley, R. J., Jones, R. F. and Brooks, S. C. (1990) Isolation and characterization of a spontaneously immortalized human breast epithelial cell line, MCF-10. Cancer Research **50**, 6075–6086.
67 Debnath, J., Muthuswamy, S. K. and Brugge, J. S. (2003) Morphogenesis and oncogenesis of MCF-10A mammary epithelial acini grown in three-dimensional basement membrane cultures. Methods **30**, 256–268.
68 Zhu, T., Gu, J., Yu, K., Lucas, J., Cai, P., Tsao, R., Gong, Y., Li, F., Chaudhary, I., Desai, P., et al. (2006) Pegylated wortmannin and 17-hydroxywortmannin conjugates as phosphoinositide 3-kinase inhibitors active in human tumor xenograft models. J. Med. Chem. **49**, 1373–1378.
69 Liu, Y., Jiang, N., Wu, J., Dai, W. and Rosenblum, J. S. (2007) Polo-like kinases inhibited by wortmannin. Labeling site and downstream effects. Journal of Biological Chemistry **282**, 2505–2511.
70 (2012) The quest for quantitative microscopy. Nat Meth, Nature Publishing Group, a division of Macmillan Publishers Limited. All Rights Reserved. **9**, 627–627.
71 Carpenter, A. E., Jones, T. R., Lamprecht, M. R., Clarke, C., Kang, I. H., Friman, O., Guertin, D. A., Chang, J. H., Lindquist, R. A., Moffat, J., et al. (2006) CellProfiler: image analysis software for identifying and quantifying cell phenotypes. Genome Biol **7**, R100.

72 Untergasser, A., Cutcutache, I., Koressaar, T., Ye, J., Faircloth, B. C., Remm, M. and Rozen, S. G. (2012) Primer3--new capabilities and interfaces. Nucleic Acids Res **40**, e115.
73 Pfaffl, M. W. (2001) A new mathematical model for relative quantification in real-time RT-PCR. Nucleic Acids Res **29**, e45.
74 Zhou, J., Zhou, Y., Cao, S., Li, S., Wang, H., Niu, Z., Chen, D., Wang, D., Lv, L., Zhang, J., et al. (2016) Multivariate logistic regression analysis of postoperative complications and risk model establishment of gastrectomy for gastric cancer: A single-center cohort report. Scand J Gastroenterol **51**, 8–15.
75 Lee, J.-H., Yom, C.-K. and Han, H.-S. (2009) Comparison of long-term outcomes of laparoscopy-assisted and open distal gastrectomy for early gastric cancer. Surg Endosc **23**, 1759–1763.
76 Kim, Y.-W., Baik, Y. H., Yun, Y. H., Nam, B. H., Kim, D. H., Choi, I. J. and Bae, J.-M. (2008) Improved quality of life outcomes after laparoscopy-assisted distal gastrectomy for early gastric cancer: results of a prospective randomized clinical trial. Ann Surg **248**, 721–727.